PROCEDURE

Dual Emission Ratio Imaging of YCs

Briefly, the procedure for time-lapse $[Ca^{2+}]_c$ imaging in cultured cells is as follows (Miyawaki et al. 2000).

1. Attach HeLa cells to a coverslip in a petri dish. Transfect cells in the dish with 1 μg of cDNA using Lipofectin (Invitrogen).
2. Between 2 and 10 days after cDNA transfection, image HeLa cells on an inverted microscope (IX70) with a cooled CCD camera (Micromax, Roper Scientific). Expose cells to reagents in HBSS containing 1.26 mM $CaCl_2$<!>.

   Note: In the authors' setup, image acquisition and processing are controlled by a personal computer connected to a camera and filter wheels (Lambda 10–2, Sutter Instruments) using the program MetaFluor (Universal Imaging). The excitation filter wheel in front of the xenon lamp and the emission filter wheel (Lambda 10-2, Sutter Instruments) immediately below the CCD camera are also under computer control. Although the excitation filter wheel can be replaced with a fixed one, the emission filter wheel is required for imaging cameleons. Excitation light from a 75-W xenon lamp is passed through a 440DF20 (440 ± 10 nm) excitation filter. The light is reflected onto the sample using a 455-nm long-pass (455DRLP) dichroic mirror. The emitted light is collected with a 40× (numerical aperture [NA]: 1.35) objective and passed through a 480 ± 15 nm or 480 ± 25 nm band-pass filter (480DF30 or 480DF50, donor channel) for ECFP, and a 535 ± 12.5-nm band-pass filter (535DF25, FRET channel) for YFP. Interference filters are from Omega Optical or Chroma Technologies.
3. Define several factors for image acquisition, including (a) excitation power, which depends on the type of light source and neutral density filter, (b) NA of the objective, (c) time of exposure to the light, (d) image acquisition interval, and (e) binning. The last three factors should be considered in terms of whether temporal or spatial resolution is pursued.
4. Choose moderately bright cells (see below). In addition, the fluorescence should be uniformly distributed in the cytosolic compartment but excluded from the nucleus, as expected for a 74-kD protein without targeting signals. Select regions of interest so that pixel intensities are spatially averaged.
5. At the end of an experiment, convert fluorescence signals into values of $[Ca^{2+}]$. R_{max} and R_{min} can be obtained in the following way. To saturate intracellular indicator with Ca^{2+}, increase the extracellular $[Ca^{2+}]$ to 10–20 mM in the presence of 1–5 μM ionomycin. Wait until fluorescence intensity reaches a plateau. Then, to deplete the Ca^{2+} indicator, wash the cells with Ca^{2+}-free medium (1 μM ionomycin, 1 mM EGTA, and 5 mM $MgCl_2$<!> in nominally Ca^{2+}-free HBSS). The in situ calibration for $[Ca^{2+}]$ uses the equation $[Ca^{2+}] = K'_d[(R-R_{min})/(R_{max}-R)]^{(1/n)}$, where K'_d is the apparent dissociation constant corresponding to the Ca^{2+} concentration at which R is midway between R_{max} and R_{min}, and n is the Hill coefficient. The Ca^{2+} titration curve of YC2.1 can be fitted using a single K'_d of 0.2 μM and a single Hill coefficient of 0.62. Therefore, use $K'_d = 0.2$ μM and $n = 0.62$ for YC2.1. Use $K'_d = 1.5$ μM and $n = 1.1$ for YC3.1, and $K'_d = 0.25$ μM and $n = 1.7$ for YC3.60.

   Caution: *See Appendix 3 for appropriate handling of materials marked with* <!>.

PRACTICAL CONSIDERATIONS

pH

pH-related artifacts were not an issue in the experiments that used HeLa cells, because agonist-induced $[Ca^{2+}]_c$ mobilization did not cause any intracellular pH changes detectable by the pH indicator, BCECF (data not shown). Correspondingly, comparisons of YC2 with YC2.1 and YC3 with YC3.1 showed no major differences in the reported $[Ca^{2+}]_c$ attributable to the difference in pH sensitivity. On the other hand, both YC2 and YC3 expressed in dissociated hippocampal neurons were perturbed by acidification following depolarization or glutamate stimulation. This problem was solved by using YC2.1 or YC3.1 (Miyawaki et al. 1999). YC2.12, YC3.12, and YC3.60 also give reliable Ca^{2+} responses over a physiological range of pH, from 6.5 to 6.2 (Nagai et al. 2004).

Concentration of Yellow Cameleons in Cells

The estimation of cameleon concentration in cells is essential for quantifying the tradeoff between optical detectability and Ca^{2+} buffering. It is important to consider the ability of various concentrations of YC3.1 to buffer Ca^{2+} transients in HeLa cells. During a 0.1-mM histamine challenge, sharp $[Ca^{2+}]_c$ transients followed by $[Ca^{2+}]_c$ oscillations can be observed in cells expressing < 200 μM YC3.1. In contrast, $[Ca^{2+}]_c$ recovers slowly to the baseline over a period of several hundred seconds, and oscillations are never observed when transfected HeLa cells expressed >300 μM YC3.1. Cameleons at cytosolic concentrations below 20 μM are too dim to give favorable SNRs with our current instruments. This limitation cannot be overcome by increasing the intensity of illumination because of YFP photochromism (see below).

Photochromism of Yellow Fluorescent Protein

If YFP is excited too strongly, its fluorescence will be reduced. This apparent bleaching is actually photochromism because the fluorescence recovers to some extent spontaneously and can be further restored by UV illumination (Dickson et al. 1997). Intense excitation of YCs also causes photochromism of the YFP moiety, which results in a decrease in the yellow:cyan emission ratio independent of Ca^{2+} change. The extent of photochromism is dependent on excitation power, numerical aperture of objective, and exposure time. Therefore, it is necessary to optimize these factors for each cell sample in order to minimize photochromism while still preserving a high SNR. Because the photochromism is partially reversible, the sampling interval is another factor that should be considered. Illumination at frequent intervals sometimes leads to a decrease in the resting ratio values of YCs. A better solution is to bin pixels at the cost of spatial resolution. The increased SNR permits the decrease in intensity of the excitation light with a neutral density filter and the observation of $[Ca^{2+}]_i$ oscillations without significant photochromism of the indicators.

Color CCD Camera

For dual-emission ratio imaging of YCs, consecutive data gathering has been described so far in this chapter; images are created by alternating filters in the emission path. For fast and simultaneous acquisition of YFP and CFP images, a color camera (Hamamatsu Photonics, C7780-22) composed of three CCD chips (RGB: red, green, and blue) and a prism may be used. The YFP and CFP images are captured by the G and B chips, respectively. In addition, to improve spatial resolution along the *z*-axis, a spinning-disk unit was placed in front of the camera. A confocal image of YC3.60-expressing HeLa cells is shown in Figure 3D. A series of ratio images in pseudo-color acquired at video rate (displayed at 16.7 Hz) shows how the increase in $[Ca^{2+}]_c$ appeared and propagated within the individual cells after stimulation with histamine.

PERICAMS

Circularly Permuted YFP

Wild-type GFP (WT-GFP) has a bimodal absorption spectrum with two peak maxima at 395 nm and 475 nm corresponding to the protonated (neutral) and deprotonated (anionic) states of the chromophore, respectively (Tsien 1998). The ionization state is modulated by a hydrogen-bond network, which is an intricate network of polar interactions between the chromophore and several surrounding amino acids. The chromophore of most GFP variants titrated with single pKa values, indicating that the internal proton equilibrium is disrupted by external pH.

Within the rigid "β-can" structure of GFP variants, Baird et al. (1999) found a site that can tolerate circular permutations, where two portions of the polypeptide are flipped around the central site. With obvious clefts in the β-can, the chromophore of circularly permuted GFPs (cpGFPs) seems to be more accessible to protons from outside the protein. The cpGFPs may be used to convert changes in the interaction between two protein domains into a change in the electrostatic potential of the

chromophore; in other words, to transduce information about the interaction into a fluorescence signal. A less pH-sensitive YFP variant, EYFP.1 (Miyawaki et al. 1999), was subjected to circular permutation. The original amino and carboxyl termini were fused via a pentapeptide linker GGSGG, and Y145 and N144 became the new amino and carboxyl termini, respectively. The resulting chimeric protein is called cpEYFP.1 (Nagai et al. 2001).

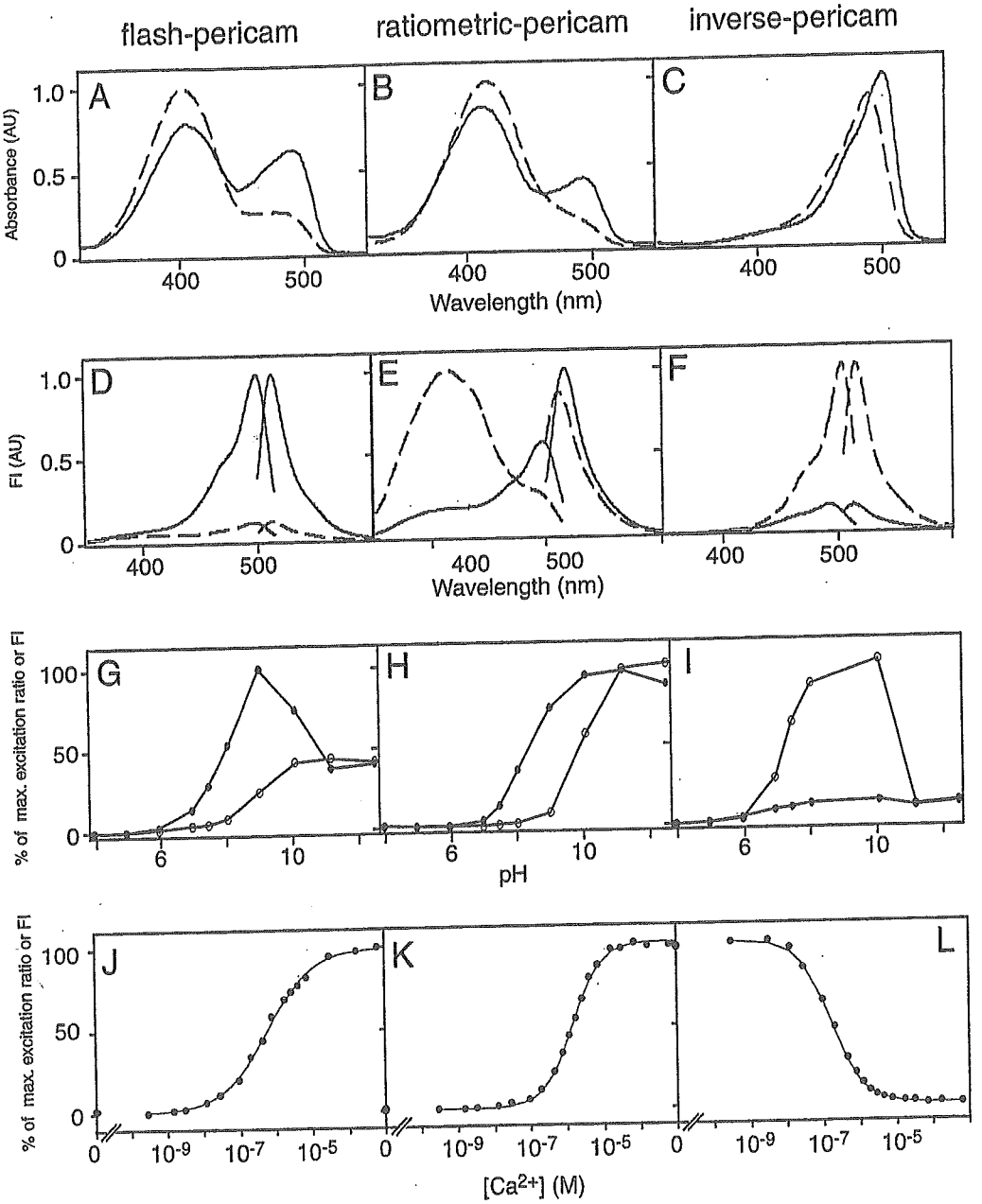

FIGURE 4. In vitro properties of flash pericam (*A*, *D*, *G*, and *J*), ratiometric pericam (*B*, *E*, *H*, and *K*), and inverse pericam (*C*, *F*, *I*, and *L*). Absorbance (*A–C*) and fluorescence excitation and emission (*D–F*) spectra of pericams. pH-dependence of normalized amplitudes in the 514-nm emission peak (*G*) and in the 516-nm emission peak (*I*) as well as the excitation ratio of 495/410 (*H*). (*A–I*) The spectra and data points were obtained in the presence (*solid circles*) or absence (*open circles*) of Ca^{2+}. (J–L) Ca^{2+} titration curves of pericams. (Fl) Fluorescence intensity. (Reprinted, with permission, from Nagai et al. 2001 [© National Academy of Sciences].)

Construction of Pericams

We first made a construct in which cpEYFP.1 was fused to the carboxyl terminus of M13 through a tripeptide linker SAG, and through a GTG linker to the amino terminus of a CaM mutant (Fig. 1B), in which the conserved bidentate glutamate at position 104 in the third Ca^{2+}-binding loop had been changed to glutamine (Miyawaki et al. 1997). As the amino terminus of CaM and the carboxyl terminus of M13 were rather far apart (58 Å when the complex was formed), the β-can of cpEYFP.1 might be considerably twisted. However, this radically designed chimeric protein was fluorescent and, as we had hoped, showed Ca^{2+} sensitivity. The protein, having a circularly *per*muted EYFP.1 and a *CaM*, was named "pericam." The CaM and M13 domains projecting from cpEYFP.1 reminded us of the bill of a pelican. When excited at 485 nm, Ca^{2+}-bound pericam showed an emission peak at 520 nm, which was three times more intense than that of Ca^{2+}-free pericam (data not shown).

Three types of pericams have been generated by mutating several amino acids adjacent to the chromophore (Fig. 4) (Nagai et al. 2001). Of these, "flash pericam" becomes bright in the presence of Ca^{2+}, similar to G-CaMP (Nakai et al. 2000), another cpGFP-based Ca^{2+} probe, whereas "inverse pericam" dims. A third pericam, "ratiometric pericam" has an excitation wavelength that changes in a Ca^{2+}-dependent manner, and thereby enables dual excitation ratiometric Ca^{2+} imaging. Ratiometric pericam realizes quantitative Ca^{2+} measurement by minimizing the effects of several artifacts that are unrelated to changes in free intracellular Ca^{2+} concentration ($[Ca^{2+}]_i$). This pericam has been successfully used to monitor changes in $[Ca^{2+}]_i$ in cardiomyocyte mitochondria (Robert et al. 2001). That report has demonstrated that mitochondrial $[Ca^{2+}]$ ($[Ca^{2+}]_m$) oscillates synchronously with cytosolic $[Ca^{2+}]$ during beating.

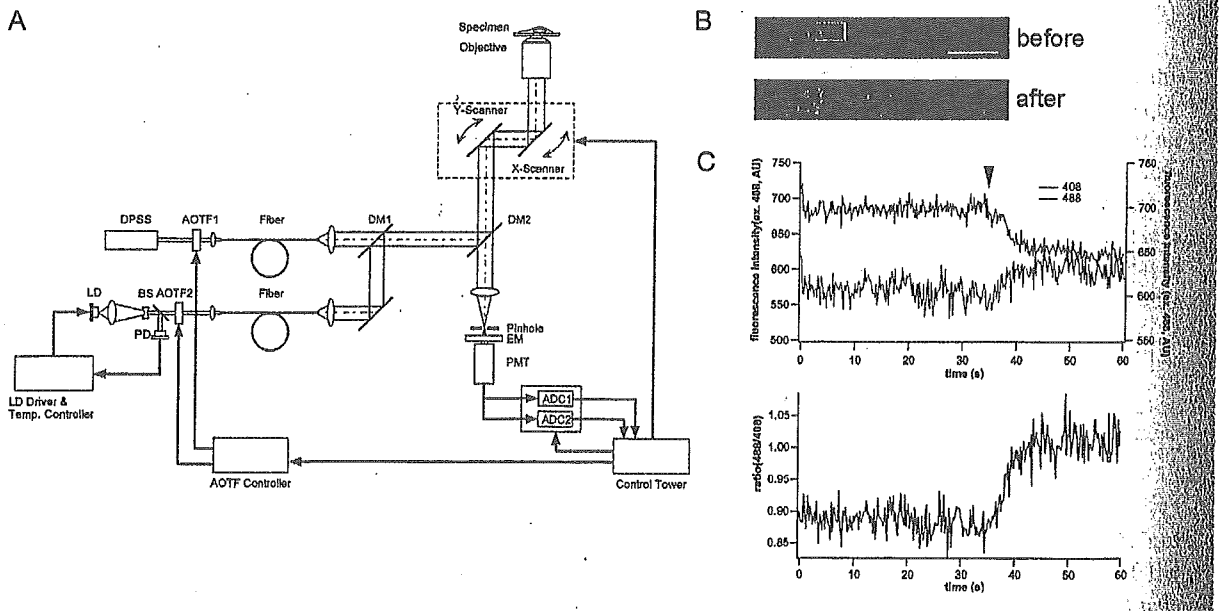

FIGURE 5. (*A*) Schematic diagram of the laser-scanning confocal microscopy system for fast dual-excitation ratiometric imaging. (DPSS) Diode-pumped solid-state laser; (LD) laser diode; (PD) photodiode; (BS) beam splitter; (DM) dichroic mirror; (EM) emission filter; (PMT) photomultiplier tube; (ADC) analog-to-digital converter. (*B*) Confocal and dual-excitation imaging of $[Ca^{2+}]_m$ using ratiometric pericam-mt. Ratio images before and after application of 1 μM histamine. Bar, 5 μm. (*C*) Time course of the averaged fluorescence signals from the white box in *B* with excitation at 488 (*green*) and 408 nm (*violet*) (*top*) and the ratio (*bottom*). The arrowhead indicates the time when histamine was applied. (Reprinted, with permission, from Shimozono et al. 2002 [©AAAS].)

Fast, Confocal Imaging of Calcium Using Ratiometric Pericam

In dual-excitation imaging, the excitation wavelength was alternated using a rotating wheel containing two band-pass filters or a high-speed grating monochromator. Use of the monochromator increased the rate at which the ratio measurement was conducted to ~10 Hz, allowing us to monitor the beat-to-beat changes in $[Ca^{2+}]_m$ of spontaneously contracting cardiac myocytes (Robert et al. 2001). These measurements were performed using conventional wide-field microscopy, which is suitable for producing the excitation peaks. However, monitoring of $[Ca^{2+}]$ change is often severely limited by the poor spatiotemporal resolution of the conventional wide-field microscopy. To obtain more reliable information on subcellular $[Ca^{2+}]$ change, it is necessary to increase the *z*-axis resolution and the rate of production and collection of the ratios of the excitation peaks. Figure 5A is a scheme for a modified laser-scanning confocal microscopy (LSCM) system for ratiometric pericam (Shimozono et al. 2002). Fast exchange between two laser beams was achieved using acousto-optic tunable filters (AOTFs). Samples were scanned on each line sequentially by a violet laser diode (408 nm) and a diode-pumped solid-state laser (488 nm). In this way, the ratios of the excitation peaks were obtained at frequencies of up to 200 Hz.

Calcium Transients in Motile Mitochondria

Although the cationic probe rhod2 has been widely used for measuring $[Ca^{2+}]_m$, the targeting specificity of this probe relies on the negative membrane potential of this organelle. On the other hand, the Ca^{2+}-sensitive photoprotein aequorin can be specifically targeted to the mitochondria and has been used for monitoring mitochondrial Ca^{2+} dynamics. However, aequorin requires the incorporation of coelenterazine, is irreversibly consumed by Ca^{2+}, and is very difficult to image because of its weak luminescence. To overcome these limitations, we have selectively targeted the ratiometric pericam to mitochondria in HeLa cells. First, changes in $[Ca^{2+}]_m$ were monitored by alternating the excitation wavelength automatically with conventional wide-field microscopy. In those studies, the excitation ratio acquisition rate was ~10 Hz, which was identical to the frame rate. Despite this high acquisition rate, the $[Ca^{2+}]_m$ measurements were often adversely affected by the rapid movement of the mitochondria, particularly at warmer temperatures. Therefore, using the modified LSCM technique, we increased the speed of excitation wavelength alteration so that it was faster than the movement of the mitochondria. With this method, the frame rate was 5 Hz and the excitation ratio-acquisition rate was 200 Hz. Although the frame rate did not allow us to fully monitor the rapid movement of the mitochondria, the high ratio-acquisition rate minimized the time lag between the two measurements used to produce each ratio signal. We believe that this $[Ca^{2+}]_m$ imaging method effectively corrects for the movement of mitochondria laterally or into and out of the optical section. After the application of histamine, spots of $[Ca^{2+}]_m$ increasing within a mitochondrion were identifiable (Fig. 5B), and the global increase in $[Ca^{2+}]_m$ was found to occur relatively slowly (Fig. 5C).

REFERENCES

Baird G.S., Zacharias D.A., and Tsien R.Y. 1999. Circular permutation and receptor insertion within green fluorescent proteins. *Proc. Natl. Acad. Sci.* **96:** 11241–11246.

Dickson R.M., Cubitt A.B., Tsien R.Y., and Moerner W.E. 1997. On/off blinking and switching behaviour of single molecules of green fluorescent protein. *Nature* **388:** 355–358.

Griesbeck O., Baird G.S., Campbell R.E., Zacharias D.A., and Tsien R.Y. 2001. Reducing the environmental sensitivity of yellow fluorescent protein. Mechanism and applications. *J. Biol. Chem.* **276:** 29188–29194.

Miyawaki A. 2003a. Fluorescence imaging of physiological activity in complex systems using GFP-based probes. *Curr. Opin. Neurobiol.* **13:** 591–596.

———. 2003b. Visualization of the spatial and temporal dynamics of intracellular signaling. *Developmental Cell* **4:** 295–305.

Miyawaki A., Griesbeck O., Heim R., and Tsien R.Y. 1999. Dynamic and quantitative Ca^{2+} measurements using improved cameleons. *Proc. Natl. Acad. Sci.* **96:** 2135–2140.

Miyawaki A., Mizuno H., Llopis J., Tsien R.Y., and Jalink K. 2000. Cameleons as cytosolic and intra-organellar calcium probes. In *Calcium Signalling: A practical approach* (ed. A.V. Tepikin), pp. 3–16. Oxford University Press, Oxford, United Kingdom.

Miyawaki A., Llopis J., Heim R., McCaffery J.M., Adams J.A., Ikura M., and Tsien R.Y. 1997. Fluorescent indicators for Ca^{2+} based on green fluorescent proteins and calmodulin. *Nature* **388:** 882–887.

Mizuno H., Sawano A., Eli P., Hama H., and Miyawaki A. 2001. Red fluorescent protein from *Discosoma* as a fusion tag and a partner for fluorescence resonance energy transfer. *Biochemistry* **40:** 2502–2510.

Nakai J., Ohkura M., and Imoto K. 2001. A high signal-to-noise Ca^{2+} probe composed of a single green fluorescent protein. *Nat. Biotechnol.* **19:** 137–141.

Nagai T., Sawano A., Park E.S., and Miyawaki A. 2001. Circularly permuted green fluorescent proteins engineered to sense Ca^{2+}. *Proc. Natl. Acad. Sci.* **98:** 3197–3202.

Nagai T., Yamada S., Tominaga T., Ichikawa M., and Miyawaki A. 2004. Expanded dynamic range of fluorescent indicators for Ca^{2+} by circularly permuted yellow fluorescent proteins. *Proc. Natl. Acad. Sci.* **101:** 10554–10559.

Nagai T., Ibata K., Park E.S., Kubota M., Mikoshiba K., and Miyawaki A. 2002. A variant of yellow fluorescent protein with fast and efficient maturation for cell-biological applications. *Nat Biotechnol.* **20:** 87–90.

Porumb T., Yau P., Harvey T.S., and Ikura M. 1994. A calmodulin-target peptide hybrid molecule with unique calcium-binding properties. *Protein Eng.* **7:** 109–115.

Robert V., Gurlini P., Tosello V., Nagai T., Miyawaki A., Di Lisa F., and Pozzan T. 2001. Beat-to-beat oscillations of mitochondrial Ca^{2+} in cardiac cells. *EMBO J.* **20:** 4998–5007.

Shimozono S., Fukano T., Nagai T., Kirino Y., Mizuno H., and Miyawaki A. 2002. Confocal imaging of subcellular Ca^{2+} concentrations using a dual-excitation ratiometric indicator based on green fluorescent protein. *Sci. STKE* **2002:** PL4. http://www.stke.org/cgi/content/full/OC_sigtrans;2002/125/pl4

Tsien R.Y. 1998. The green fluorescent protein. *Annu. Rev. Biochem.* **67:** 509–544.

———. 2000. Physiological indicators based on fluorescence resonance energy transfer. In *Imaging neurons: A laboratory manual* (ed. R. Yuste et al.), pp. 55.1–55.10. Cold Spring Harbor Laboratory Press, Cold Spring Harbor, New York.

THE JOURNAL OF BIOLOGICAL CHEMISTRY
Vol. 280, No. 7, Issue of February 18, pp. 5764–5772, 2005
Printed in U.S.A.

Calcineurin Inhibits Na^+/Ca^{2+} Exchange in Phenylephrine-treated Hypertrophic Cardiomyocytes*

Received for publication, September 7, 2004, and in revised form, November 4, 2004
Published, JBC Papers in Press, November 22, 2004, DOI 10.1074/jbc.M410240200

Yuki Katanosaka‡§, Yuko Iwata‡, Yuko Kobayashi‡, Futoshi Shibasaki¶, Shigeo Wakabayashi‡, and Munekazu Shigekawa‡‖**

From the ‡Department of Molecular Physiology, National Cardiovascular Center Research Institute, Fujishiro-dai 5-7, Suita, Osaka 565-8565, the ¶Department of Molecular Cell Physiology, The Tokyo Metropolitan Institute of Medical Science, Honkomagome 3-18-22, Bunkyo-ku, Tokyo 113-8613, and the ‖Department of Human Life Sciences, Senri-Kinran University, Fujishiro-dai 5-25-1, Suita, Osaka 565-0873 Japan

The cardiac Na^+/Ca^{2+} exchanger (NCX1) is the predominant mechanism for the extrusion of Ca^{2+} from beating cardiomyocytes. The role of protein phosphorylation in the regulation of NCX1 function in normal and diseased hearts remains unclear. In our search for proteins that interact with NCX1 using a yeast two-hybrid screen, we found that the C terminus of calcineurin Aβ, containing the autoinhibitory domain, binds to the β1 repeat of the central cytoplasmic loop of NCX1 that presumably constitutes part of the allosteric Ca^{2+} regulatory site. The association of NCX1 with calcineurin was significantly increased in the BIO14.6 cardiomyopathic hamster heart compared with that in the normal control. In hypertrophic neonatal rat cardiomyocytes subjected to chronic phenylephrine treatment, we observed a marked depression of NCX activity measured as the rate of Na^+_i-dependent $^{45}Ca^{2+}$ uptake or the rate of Na^+_o-dependent $^{45}Ca^{2+}$ efflux. Depressed NCX activity was partially and independently reversed by the acute inhibition of calcineurin and protein kinase C activities with little effect on myocyte hypertrophic phenotypes. Studies of NCX1 deletion mutants expressed in CCL39 cells were consistent with the view that the β1 repeat is required for the action of endogenous calcineurin and that the large cytoplasmic loop may be required to maintain the interaction of the enzyme with its substrate. Our data suggest that NCX1 is a novel regulatory target for calcineurin and that depressed NCX activity might contribute to the etiology of *in vivo* cardiac hypertrophy and dysfunction occurring under conditions in which both calcineurin and protein kinase C are chronically activated.

The Na^+/Ca^{2+} exchanger (NCX)[1] catalyzes the reversible exchange of Na^+ for Ca^{2+} across the plasma membrane. In normal cardiac muscle, the primary role of NCX1 (the cardiac isoform of NCX) is to extrude cytoplasmic Ca^{2+} during myocyte repolarization and diastole, which balances Ca^{2+} entry via L-type Ca^{2+} channels during myocyte depolarization (1, 2). The transport activity of NCX1 is known to be influenced by a variety of factors, including hormones and growth factors, intracellular Na^+ and Ca^{2+} concentrations, membrane potential, cytoplasmic ATP, and protein and lipid phosphorylation (3). However, information is still limited as to the quantitative aspects of changes in these factors and their consequences on NCX1 activity in normal and diseased cardiomyocytes. For example, in hypertrophic and failing hearts from human patients and animal models, sarcolemmal NCX1 expression has often been shown to be elevated (4–7), which could be compensatory for the reduced ability of the sarcoplasmic reticulum to maintain low diastolic $[Ca^{2+}]_i$ under these pathological conditions. However, whether increased NCX expression invariably leads to enhanced function under disease conditions is not clear, although enhanced NCX expression and function have been observed in cardiomyocytes isolated from some animal models of cardiac hypertrophy and heart failure (6, 7).

Protein phosphorylation is an important mechanism regulating the functions of many cellular systems. In the case of NCX1, acute treatment with PMA or agonists of $G\alpha_q$-coupled receptors such as phenylephrine (PE) has been shown to enhance NCX activity in isolated cardiomyocytes as well as in cells expressing cloned NCX1 (8–10). Protein kinase A activation has also been reported to stimulate NCX1 activity (11, 12). On the other hand, a protein phosphatase inhibitor, calyculin A, reportedly causes substantial inhibition of NCX activity in cells expressing cloned NCX1 (13). NCX1 stimulation by PMA and agonists of $G\alpha_q$-coupled receptors occurs via a mechanism involving PKC activation and requires the participation of the central cytoplasmic loop of the exchanger (see Fig. 1*a*) (9). Because these agonist effects did not require the direct phosphorylation of NCX1, the central cytoplasmic loop was considered to serve as an anchor for phosphorylatable regulatory ancillary protein(s) (9).

In this study, we undertook a search for regulatory proteins interacting with the central cytoplasmic loop of NCX1 by using a yeast two-hybrid screen. From this search and subsequent analysis, we identified a complex, hitherto unrecognized regulatory mechanism for cardiac NCX1 involving calcineurin and PKC in hypertrophic cardiomyocytes subjected to prolonged PE pretreatment. This mechanism is capable of markedly depressing NCX1 activity. Because calcineurin acts as a central medi-

* This work was supported by Special Coordination Funds from the Ministry of Education, Culture, Sports, Science and Technology, a Grant for Promotion of Fundamental Studies in Heath Science from the Organization of Pharmaceutical Safety and Research, and a grant from the Uehara Foundation. The costs of publication of this article were defrayed in part by the payment of page charges. This article must therefore be hereby marked "*advertisement*" in accordance with 18 U.S.C. Section 1734 solely to indicate this fact.

§ Research Fellow of the Japan Society for the Promotion of Science.
** To whom correspondence should be addressed. Tel.: 81-6-6872-7846; Fax: 81-6-6872-7872; E-mail: shigekaw@ri.ncvc.go.jp.

[1] The abbreviations used are: NCX, Na^+/Ca^{2+} exchanger; NCX1, cardiac isoform of NCX; aa, amino acids; ANP, atrial natriuretic peptide; BSS, balanced salt solution; CnA, calcineurin A; DOX, doxycycline; FCS, fetal calf serum; PE, phenylephrine; PKC, protein kinase C; PMA, phorbol 12-myristate 13-acetate; Rp-8-CPT-cAMPS, 8-(4-chlorophenylthio)adenosine-3′,5′-cyclic monophosphorothioate; Rp-8-CPT-cGMPS, 8-(4-chlorophenylthio)guanosine-3′,5′-cyclic monophosphorothioate; TUNEL, terminal deoxynucleotidyltransferase-mediated dUTP nick end-labeling.

ator of *in vivo* cardiac hypertrophy and failure (14–16), NCX might contribute to the etiology of *in vivo* cardiac dysfunction.

EXPERIMENTAL PROCEDURES

Materials—FCS, PE, FK506, PMA, calphostin C, 8-bromo-cAMP, Rp-8-CPT-cAMPS, 8-bromo-cGMP, Rp-8-CPT-cGMPS, and H89 were purchased from Sigma. GF109203X, chelerythrine chloride, KN93, and KN62 were purchased from Calbiochem. Rhodamine-conjugated phalloidin was obtained from Molecular Probes. Antibodies to NCX isoforms have been described (8, 9). Rabbit polyclonal anti-pan calcineurin A (CnA) and goat polyclonal anti-CnAβ (Santa Cruz Biotechnology), mouse monoclonal anti-CnAβ (Upstate Technology), anti-hemagglutinin (Roche Applied Science), rabbit polyclonal anti-atrial natriuretic peptide (anti-ANP; Phoenix Pharmaceuticals), fluorescein isothiocyanate-conjugated anti-rabbit IgG and rhodamine-conjugated anti-goat IgG (ICN/CAPEL), and anti-calmodulin, horseradish peroxidase-conjugated anti-rabbit IgG, and biotin-conjugated anti-mouse IgG (Zymed Laboratories Inc.) were purchased the from the sources indicated in parentheses. Horseradish peroxidase-conjugated streptavidin was obtained from Zymed Laboratories Inc.. $^{45}CaCl_2$ was purchased from Amersham Biosciences.

Animals—Pregnant Wister rats and male Bio14.6 hamsters (J2N-k strain, 120 days old) and age-matched normal controls (J2N-n) were purchased from Japan SLC. The J2N-n had the same genetic background as the J2N-k, except for the difference of a genetic locus for cardiomyopathy.

Cell Cultures—Primary cardiomyocyte cultures were prepared from ventricles of 1-day-old rats as described previously (17). They were plated on collagen-coated 24-well dishes at a density of 4×10^6 cells per well and maintained in M199 medium supplemented with 10% FCS. Staining with rhodamine-phalloidin revealed that >90% of the cells were cardiomyocytes. Two days later, the cells were divided into three groups and then maintained for up to 5 days in M199 alone, M199 with 10 μM PE, or M199 with 10% FCS (see Fig. 3*a*). These myocytes usually form clusters and exhibit spontaneous synchronized beating (17). On the other hand, CCL39 cells (American Type Culture Collection) and their NCX1 transfectants were maintained in Dulbecco's modified Eagle's medium containing 7.5% FCS, 50 units/ml penicillin, and 50 μg/ml streptomycin.

Construction of Vectors and Expression of NCX1 and Calcineurin—The preparation of cDNAs of dog heart NCX1 and NCX1 mutants lacking aa 246–672 (NCX1Δ246–672) or aa 407–478 (NCX1Δ407–478), their transfection into CCL39 cells, and the isolation of cell clones stably expressing high NCX activity were carried out as described previously (8, 9). The isolation of cDNA encoding human CnAβ and the construction of its constitutively active mutant (ΔCnA) lacking the autoinhibitory and the calmodulin binding domains were described previously (18, 19). A catalytically inactive mutant of CnA that functions as a dominant negative mutant was prepared from ΔCnA by mutating histidine at position 160 to glutamine (19). Hemagglutinin-tagged wild-type and mutant CnAβs were subcloned into an adenoviral vector downstream of the Tet-Off system (18). Cardiomyocytes were infected with adenoviral vectors at a multiplicity of infection of 100 plaque-forming units per cell in serum-free M199 medium for 2 h at 37 °C. Efficiency of infection under these conditions was 100%, as revealed by immunostaining with an anti-hemagglutinin antibody. In control cells, the expression of adenoviral vectors was suppressed with 1 μM doxycycline (DOX) added to culture medium.

Yeast Two-hybrid Screen—We used Matchmaker 3 (Clontech) for the yeast two-hybrid screen. DNA fragments corresponding to the following segments of the central cytoplasmic loop of dog NCX1, shown in Fig. 1*a*, were prepared using a PCR-based method: the NCX inhibitory peptide (*XIP*, Fig. 1*a*), aa 250–406; β1, aa 407–478; β1-β2, aa 479–538; β2, aa 539–613; C terminus (*CT*, Fig. 1*a*), aa 614–796; N terminus (*NT*, Fig. 1*a*), aa 250–613; and the full loop (*Full*, Fig. 1*a*), aa 250–796. Each DNA fragment was fused to the GAL4 DNA binding domain in the pGBKT7 vector. We used a mixture of yeasts carrying each of these bait constructs for the initial screening of ~4×10^7 clones from a human brain cDNA library fused to the GAL4 activation domain. These bait and library yeast strains were mated by culturing on agar plates in complete YPD (1% yeast extract, 2% peptone, and 2% glucose) medium overnight at 20 °C. After successive screening in medium lacking histidine, leucine, and tryptophan (−*HLT*, Fig. 1*b*) and then in medium lacking histidine, adenine, leucine, and tryptophan (−*HALT*, Fig. 1*b*), grown-up colonies were isolated and subjected to β-galactosidase assay according to the manufacturer's instructions. The inserts in β-galactosidase-positive clones were sequenced using the activation domain sequence primers by the ABI 9600 sequencer. Positive clones were verified by one-on-one transformations and selections by growth on agar plates in −HALT medium and β-galactosidase assay (see Fig. 1*b*).

Immunoprecipitation, Immunoblot, and Immunocytochemical Analyses—Brain and/or ventricular tissues from rat or hamster and cultured rat cardiomyocytes were homogenized by Hiscotron (NITI-ON, Funabashi, Japan) in radioimmune precipitation assay lysis buffer containing 20 mM HEPES (pH 7.4), 150 mM NaCl, 1% sodium deoxycholate, 1% Triton X-100, 0.1% SDS, 2 μg/ml leupeptin, 1 μg/ml aprotinin, 200 μM phenylmethylsulfonyl fluoride, and 200 μM benzamidine hydrochloride. The lysates were subjected to centrifugation at 100,000 × *g* for 20 min, and the resultant supernatant (up to 5 mg protein) was pre-cleared with 50 μl of protein A-Sepharose beads for 2 h at 4 °C on a rotator. After centrifugation, the supernatant was incubated with anti-pan CnA for 2 h at 4 °C and then with 50 μl of protein A-Sepharose beads for at least 2 h at 4 °C on a rotator. The beads were washed eight times with ice-cold phosphate-buffered saline. Proteins solubilized from beads by boiling in the Laemmli buffer (20) were subjected to SDS-PAGE on a 8.5% gel and then to immunoblotting with an appropriate antibody. Immunoblot analysis was performed essentially as described previously (21). The immunoblot was visualized using an enhanced chemiluminescence detection system (Amersham Biosciences).

For immunocytochemistry, 5-μm-thick sections of normal and BIO14.6 hamster ventricular tissues embedded in OCT compound (Tissue-Tek) were permeabilized with 0.1% Triton X-100 and treated with rabbit polyclonal anti-NCX1 or goat polyclonal anti-CnAβ at dilutions of 1:500 and 1:200, respectively. These samples were then treated with fluorescein isothiocyanate-conjugated anti-rabbit IgG or rhodamine-conjugated anti-goat IgG. For immunostaining of rat cardiomyocytes, cells immobilized on collagen-coated glass slides were fixed with 4% paraformaldehyde for 15 min at room temperature, permeabilized with 0.1% Triton X-100, and then stained with anti-NCX1, anti-pan CnA, or anti-ANP. For double staining with a combination of polyclonal (rabbit) and monoclonal (mouse) antibodies, fixed and permeabilized myocytes were incubated with a mixture of two primary antibodies and then with a mixture of the fluorescence-labeled anti-mouse and rhodamine-labeled anti-rabbits IgGs. Cells were examined by a confocal laser scanning microscopy (MRC-1024, Bio-Rad) mounted on an Olympus BX50WI epifluorescence microscope with a plan-apochromat 60× water immersion objective lens (Olympus).

Fractionation of Heart Extracts—Normal and BIO14.6 hamster hearts were homogenized in phosphate-buffered saline using a Hiscotron homogenizer and centrifuged at 15,000 × *g* for 15 min. The resultant supernatant was centrifuged at 500,000 × *g* for 45 min to yield supernatant and pellet fractions. Most of the sarcolemmal and sarcoplasmic reticulum membranes were presumably recovered in the pellet fraction. Both the supernatant and pellet fractions were then subjected to immunoblot analysis with anti-pan CnA.

Na^+_i-dependent $^{45}Ca^{2+}$ Uptake into and Na^+_o-dependent $^{45}Ca^{2+}$ Efflux from Cells—Na^+_i-dependent $^{45}Ca^{2+}$ uptake into cells was measured as described previously (8, 9, 22) with slight modifications. Cardiomyocytes or CCL39 cells cultured in 24-well dishes were loaded with Na^+ by incubating them at 37 °C for 30 min in 0.5 ml of normal BSS (10 mM Hepes/Tris (pH7.4), 146 mM NaCl, 4 mM KCl, 2 mM $MgCl_2$, 0.1 mM $CaCl_2$, 10 mM glucose, and 0.1% bovine serum albumin) containing 1 mM ouabain and 10 μM monensin. In cardiomyocytes pretreated with PE or FCS, Na^+ loading was carried out during the last 30 min of such pretreatment. $^{45}Ca^{2+}$ uptake was then initiated by switching the medium to Na^+-free BSS containing choline chloride or to normal BSS, both of which contained 370 kBq of $^{45}Ca^{2+}$ and 1 mM ouabain. After a 30-s incubation, cells were washed with an ice-cold solution containing 10 mM $LaCl_3$ to stop $^{45}Ca^{2+}$ uptake. Cells were subsequently solubilized with 0.1 N NaOH, and aliquots were taken for the determination of radioactivity and protein. Na^+_i-dependent $^{45}Ca^{2+}$ uptake was estimated by subtracting $^{45}Ca^{2+}$ uptake in normal BSS from that in Na^+-free BSS. To observe the effects of FK506, protein kinase modulators, or thapsigargin, cells were incubated with these substances during the last 15–30 min of Na^+ loading, except that endogenous PKC was down-regulated by treatment with 0.3 μM PMA for 24 h. The Na^+_i-dependent $^{45}Ca^{2+}$ uptake activities in control cells not pretreated with PE or other agents were as follows: for cardiomyocytes, 12.1 ± 0.5 nmol/mg/30s (n = 9); for CCL39 cells expressing the wild-type NCX1, NCX1Δ246–672, and NCX1Δ407–478, 10.4 ± 0.5, 4.2 ± 0.4, and 5.3 ± 0.2 nmol/mg/30s (n = 9), respectively. These values were taken as 100% in Figs. 3*d*, 4*a*, 5, 6, and 7.

To measure $^{45}Ca^{2+}$ efflux, cardiomyocytes in 35-mm dishes were incubated in 1 ml BSS containing 740 kBq of $^{45}Ca^{2+}$ for the last 2 and

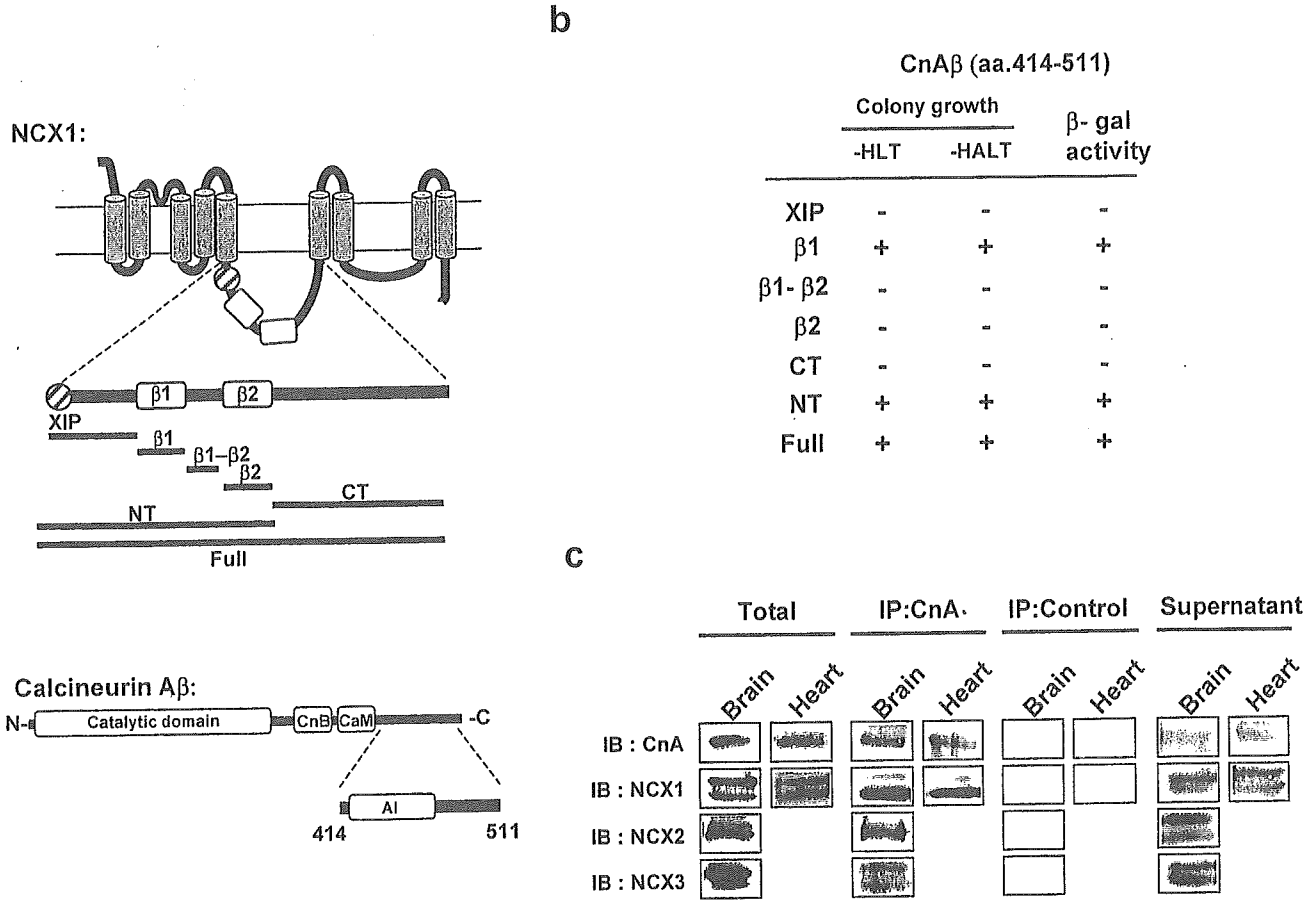

FIG. 1. **Identification of CnAβ as a NCX-binding protein.** *a*, domain structures of NCX1 and CnAβ. Segments of the central cytoplasmic loop of NCX1, labeled as indicated (*XIP*, NCX inhibitory peptide; *NT*, N terminus; *CT*, C terminus), were used as bait for the yeast two-hybrid screen. In CnAβ, *CnB*, *CaM*, and *AI* are the calcineurin B binding, the calmodulin binding, and the autoinhibitory domains, respectively. *b*, colony growth after one-on-one transformation and selection in medium lacking histidine, leucine, and tryptophan (*−HLT*) or medium lacking histidine, alanine, leucine, and tryptophan (*−HALT*) and β-galactosidase (*β-gal*)-positive colonies in −HALT medium. *c*, co-immunoprecipitation of CnA with NCX isoforms. Lysates from rat brain and heart (*Total*), materials immunoprecipitated with anti-pan CnA (*IP:CnA*) or no antibody (*IP:control*), and post-immunoprecipitation supernatants (*Supernatant*) were subjected to immunoblot (*IB*) assays with antibodies to the indicated proteins.

4 h of the 72-h treatment with and without 10 μM PE, respectively, which produced essentially the same level of $^{45}Ca^{2+}$ loading in PE-treated and non-treated cells. After rinsing cells six times with Ca^{2+}- and Na^+-free BSS for 1 min, $^{45}Ca^{2+}$ efflux was measured for 20 s in Ca^{2+}- and Na^+-free BSS or in Ca^{2+}-free BSS, both of which contained 1 μM thapsigargin, to acutely increase $[Ca^{2+}]_i$ (23). Na^+_o-dependent $^{45}Ca^{2+}$ efflux was estimated by subtracting $^{45}Ca^{2+}$ efflux in Ca^{2+}- and Na^+-free BSS from that in Ca^{2+}-free BSS.

Detection of TUNEL-positive Cells—For *in situ* detection of DNA fragmentation, we assayed TUNEL-positive cells using an apoptosis detection kit (Takara Biomedical) essentially as described previously (24). The number of TUNEL-labeled nuclei was counted by observing rat cardiomyocytes with a light microscope (40× objective; Olympus). TUNEL-positive cells were <3% in normal cardiomyocytes.

Data Analysis—Reproducibility of the data presented in the figures and those described in the text was confirmed in at least three independent experiments. Significant differences between two groups of data were evaluated by an analysis of variance assay with *post hoc* tests. $p < 0.05$ was considered as a statistically significant finding.

RESULTS

Isolation of CnAβ as a NCX1-binding Protein and Mapping of the Interacting Site in NCX1—To isolate protein(s) interacting with NCX1, we performed the yeast two-hybrid screen of a human brain cDNA library using various segments of the large central loop of NCX1 as bait (Fig. 1*a*). From an initial screen in which we used a mixture of yeast populations expressing individual bait sequences, we isolated a positive clone encoding a ~100 amino acid C-terminal tail of CnAβ with its autoinhibitory domain (Fig. 1*a*). We then examined the interaction of individual NCX segments with the CnAβ tail by one-on-one transformations and selection by colony growth and β-galactosidase assays (Fig. 1*b*). We confirmed that aa 407–478 of the NCX1 protein, known as the β1 repeat, and other fragments containing this same sequence associate with the CnAβ tail.

We examined whether calcineurin interacts with NCX1 and its isoforms (NCX2 and NCX3) at the protein level. We found that anti-pan CnA co-precipitated proteins reactive with antibody to each isoform from lysates of rat brain and heart, although these proteins were still relatively abundant in the supernatant fractions (Fig. 1*c*). Thus, at least some calcineurin was physically associated with NCX isoforms, consistent with the fact that the β1 repeat sequence is conserved in these isoforms. Of note, anti-pan CnA immunoprecipitated single major proteins from rat (Fig. 1*c*) and hamster (Fig. 2*b*) hearts that were recognized by anti-CnAβ, indicating that the antibody predominantly precipitated CnAβ under the conditions used.

Enhanced Association of CnAβ with NCX1 in BIO14.6 Hamster Heart—The BIO14.6 hamsters develop cardiomyopathy and muscular dystrophy due to δ-sarcoglycan deficiency (25, 26). We examined the interaction of NCX1 with calcineurin in the hearts of 120-day-old BIO14.6 hamsters, because our recent study has suggested that $[Ca^{2+}]_i$ might be elevated in BIO14.6 cardiomyocytes due to increased basal Ca^{2+} influx (27). Anti-CnAβ immunoprecipitated more abundant NCX1

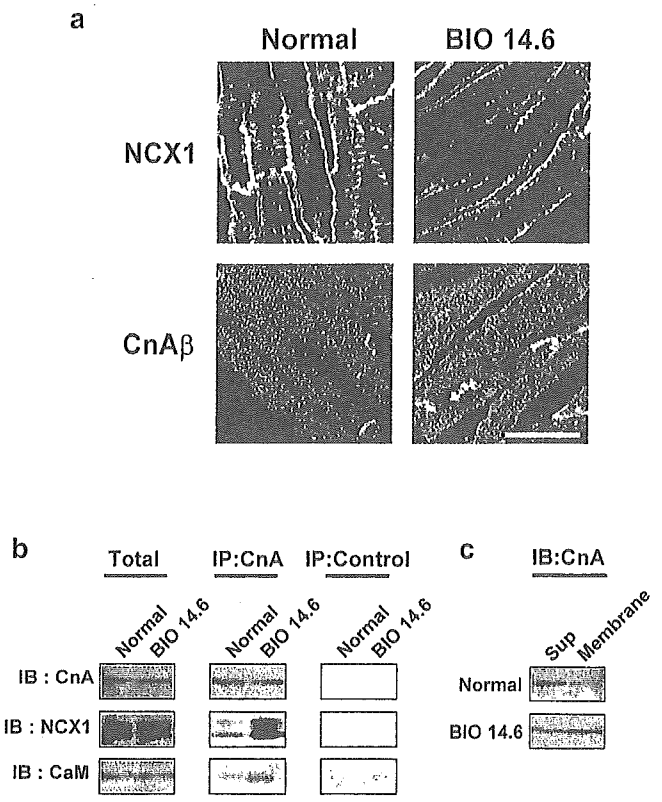

FIG. 2. **Subcellular localization of NCX1 and CnAβ in normal and BIO14.6 hamster hearts.** *a*, immunostaining of hamster ventricular muscle with anti-NCX1 or anti-CnAβ. *Bar*, 20 μm. *b*, co-immunoprecipitation of NCX1 and calmodulin (*CaM*) with CnA. Lysates of normal and BIO14.6 hamster ventricular muscles (*Total*) and materials immunoprecipitated with anti-pan CnA (*IP:CnA*) or no antibody (*IP: control*) were subjected to immunoblot analyses with antibodies to the indicated proteins. *c*, subcellular fractionation of normal and BIO14.6 hamster ventricular homogenates followed by immunoblot (*IB*) assays of membrane and supernatant (*Sup*) fractions with anti-pan CnA.

protein from BIO14.6 than from normal hearts despite the similar contents of NCX1 and calcineurin in these preparations (Fig. 2*b*).

Interestingly, calmodulin also was more abundant in the immunoprecipitates from BIO14.6 heart, although total calmodulin was again not different (Fig. 2*b*), suggesting that calcineurin is activated in the BIO14.6 heart. Immunocytochemistry with anti-CnAβ revealed the presence of calcineurin at the peripheral sarcolemma in BIO14.6 but not in normal cardiomyocytes, although it was detectable in the cell interior and at the intercalated discs in both types of myocytes (Fig. 2*a*). Striated patterns seen in the cell interior may reflect the presence of calcineurin in the Z-lines (16). Furthermore, calcineurin was more abundant in the membrane *versus* the cytosolic fraction prepared from the BIO14.6 heart, whereas the opposite was true of normal heart muscle (Fig. 2*c*). Thus, the association of calcineurin with NCX1 is significantly enhanced in BIO14.6 compared with normal hearts.

NCX Activity Is Regulated by Calcineurin in Rat Cardiomyocytes or CCL39 Cells Expressing Cloned NCX1—To examine the possible effects of calcineurin on NCX activity, we used rat neonatal cardiomyocytes subjected to pretreatment with 10 μM PE for 72 h (see protocol in Fig. 3*a*). In these myocytes, a prominent increase in cell size with enhanced sarcomere organization and enhanced expression of ANP was observed (Fig. 3*b*) (14, 17, 28). The NCX1 protein was detectable in the sarcolemma, particularly in the intercellular junctions (Fig. 3, *b* and *c*), and its expression greatly increased during the PE treatment, although calcineurin expression remained essentially unchanged (Fig. 3*d*, *top*). We observed overlapping localization of NCX1 and calcineurin in the sarcolemma of myocytes after a 72-h PE treatment, consistent with the finding that a much larger amount of NCX1 protein was recovered in the anti-CnA immunoprecipitates from the PE-treated *versus* non-treated myocytes (Fig. 3*c*). These myocytes did not show a sign of apoptosis, because the number of TUNEL-positive cells was <3% the amount in non-treated control myocytes. Importantly, the rate of Na^+_i-dependent $^{45}Ca^{2+}$ uptake measured as activity per milligram of cell protein was markedly decreased in myocytes after a 72-h PE treatment (Fig. 3*d*, *bottom*). The uptake rate in the latter myocytes would be even smaller if it was normalized to cell NCX1 content (see above). On the other hand, the uptake rate was modestly increased in myocytes after a 24-h PE treatment. This uptake increase may be attributable to the increased NCX1 expression seen at this time point (Fig. 3*d*, *top*).

Intriguingly, when myocytes were treated with 0.01–1 μM the calcineurin inhibitor FK506 during the last 15–30 min of the 72-h PE treatment, the rate of Na^+_i-dependent $^{45}Ca^{2+}$ uptake increased 2-fold (Fig. 4*a*). Qualitatively similar results were obtained with myocytes pretreated with 10% FCS (Fig. 4*a*). Of note, the rate of Na^+_i-dependent $^{45}Ca^{2+}$ uptake also increased by 188 ± 3% (n = 3) when 10 μM cyclosporin A, another calcineurin inhibitor, was added to the PE-treated myocytes. On the other hand, FK506 also enhanced the rate of Na^+_o-dependent Ca^{2+} efflux from PE-pretreated cardiomyocytes (Fig. 4*b*). In this experiment, we loaded PE-treated and non-treated myocytes with $^{45}Ca^{2+}$ to equivalent levels of radioactivity, and $^{45}Ca^{2+}$ efflux was then initiated by acutely raising $[Ca^{2+}]_i$ with thapsigargin under physiological ionic conditions. These data indicate that PE and FK506 regulate both the influx and efflux modes of NCX activity.

To confirm the involvement of calcineurin in NCX regulation, we tested the effect of the adenoviral infection of dominant negative or activated CnA on cardiomyocytes pretreated with PE or FCS for up to 96 h (see Fig. 3*a*). Like FK506, dominant negative CnA, when infected at 72 h after the start of PE treatment, caused a large increase in the rate of Na^+_i-dependent $^{45}Ca^{2+}$ uptake without an appreciable change in the size of the hypertrophic myocytes (Fig. 5). On the other hand, when infected at 24 h after the start of the 72-h PE or FCS treatment, dominant negative CnA nearly prevented the occurrence of the PE- and FCS-induced uptake inhibition and severely depressed myocyte enlargement, whereas it exerted no effects on controls not pretreated with growth factors (Fig. 5 and data not shown). Under similar conditions, activated CnA significantly increased the size of control myocytes as reported previously (28, 29) and reduced the uptake rate in these cells by ~40% (Fig. 5). Furthermore, activated CnA promoted the FCS-induced uptake inhibition, although it exerted little additional effect on PE-treated myocytes. Thus, a significant portion of NCX inhibition occurring in PE- or FCS-pretreated myocytes is due to the enzymic activity of calcineurin.

We next examined the effects of protein kinase modulators on the rate of Na^+_i-dependent Ca^{2+} uptake in chronically PE-treated myocytes. Incubation of myocytes with 0.3 μM PMA during the last 30 min of a 72-h PE treatment caused little effect on the uptake rate (Fig. 6), whereas it produced a 20–30% increase in non PE-pretreated controls (data not shown), consistent with a previous report (9). In contrast, incubation with PMA during the final 24 h of a 72-h PE treatment caused an increase in the uptake rate similar to that seen at 1 μM FK506. The latter PMA effect (PKC down-regulation) was mimicked by a 30-min treatments with PKC inhibitors; the uptake rate in the presence of 0.3 μM calphostin C (Fig. 6), 50

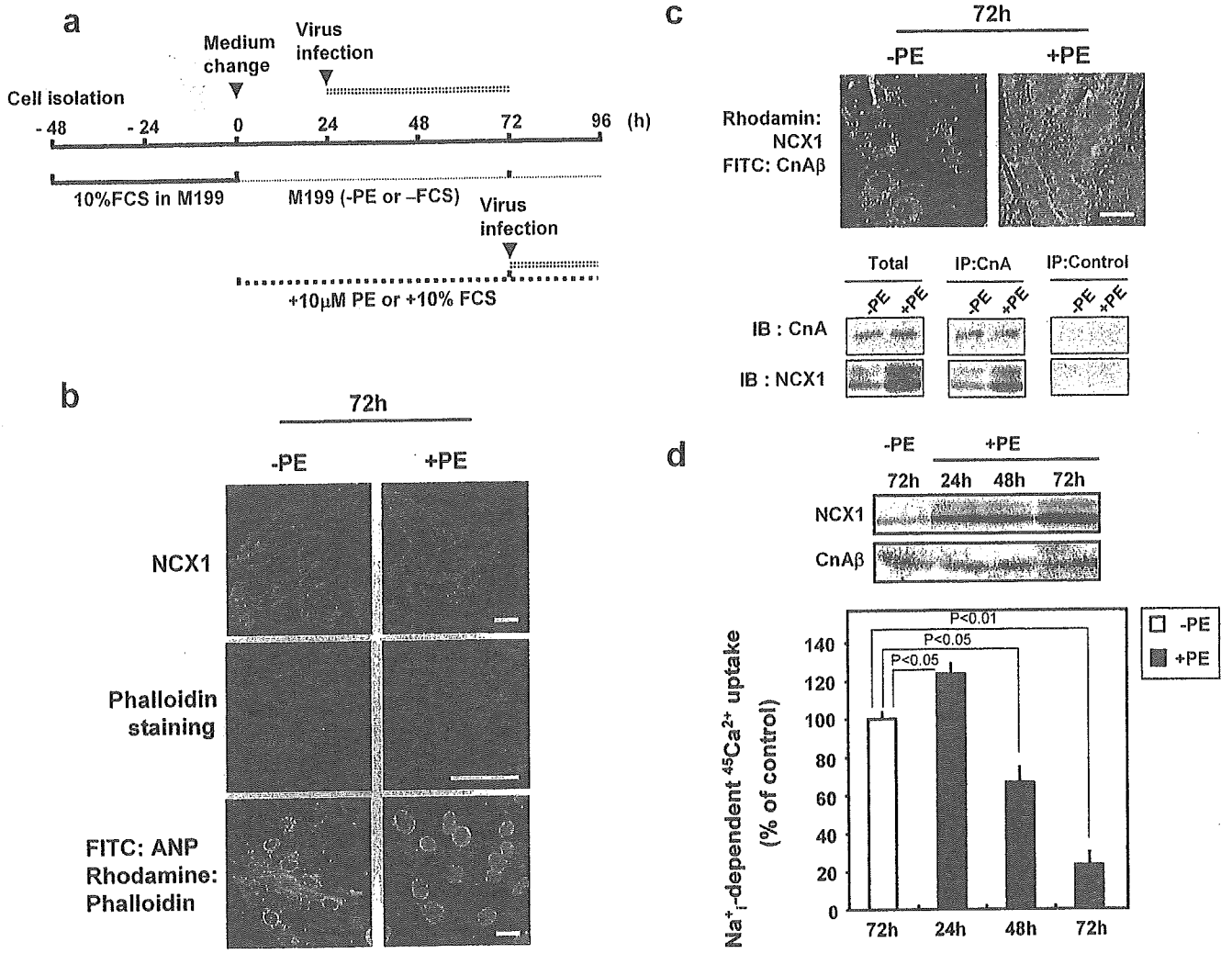

FIG. 3. **Effects of PE treatment on morphology, NCX1 and calcineurin expressions, and Na^+_i-dependent $^{45}Ca^{2+}$ uptake in cardiomyocytes.** *a*, protocol for the treatment of cardiomyocytes with PE and other agents. *b*, characterization of cardiomyocytes after a 72-h treatment with 0 (*−PE*) or 10 μM (*+PE*) PE. *Bar*, 20 μm. *Top*, immunostaining with anti-NCX1; *middle*, sarcomere assembly of myocytes visualized with rhodamine-phalloidin; *bottom*, immunostaining of myocytes with anti-ANP (*green*) and rhodamine-phalloidin (*red*). *FITC*, fluorescein isothiocyanate. *c*, co-localization and association of NCX1 and calcineurin in cardiomyocytes pretreated with PE for 72 h. *Top*, images of PE-treated or non-treated myocytes double-stained with anti-NCX1 (*red*) and anti-CnAβ (*green*). Overlapping stain is shown by *yellow* and *orange colors*. *Bar*, 20 μm. *Bottom*, lysates of PE-treated and non-treated myocytes (*Total*) and materials immunoprecipitated with anti-pan CnA (*IP:CnA*) or no antibody (*IP:control*) were subjected to immunoblot (*IB*) assay with anti-NCX1 or anti-pan CnA. *d*, time-dependent changes in the expression of NCX1 and CnAβ and the rate of Na^+_i-dependent $^{45}Ca^{2+}$ uptake (average ± S.D.; $n = 3$) in cardiomyocytes during treatment with 0 or 10 μM PE.

nM GF109203X, or 1 μM chelerythrine increased by 327 ± 4 ($n = 3$), 300 ± 6 ($n = 3$), and 296 ± 5% ($n = 3$), respectively, as compared with that of PE-treated myocytes. The effects of FK506 and 24-h PMA treatment or calphostin C were additive, suggesting that the enzymic activities of calcineurin and PKC contributed independently to the observed reduction of uptake activity in PE-treated myocytes. Under similar conditions, however, the protein kinase A activator 8-bromo-cAMP (100 μM), the protein kinase A inhibitors Rp-8-CPT-cAMPS (100 μM) and H89 (50 μM), the protein kinase G activator 8-bromo-cGMP (100 μM), the protein kinase G activator inhibitor Rp-8-CPT-cGMPS (100 μM), and the calmodulin-dependent protein kinase II inhibitors KN62 (25 μM) and KN93 (25 μM) did not influence the uptake rate (Fig. 6 and data not shown).

Finally, using CCL39 cells expressing NCX1 variants, we examined the possible role of the central cytoplasmic loop of the exchanger in the reversal of NCX inhibition by the inhibitors of calcineurin and PKC. In cells expressing wild-type NCX1 infected with activated CnA for 48 h, the rate of Na^+_i-dependent $^{45}Ca^{2+}$ uptake was 40% lower compared with that for control cells in which expression of activated CnA had been suppressed with DOX (Fig. 7*a*). Importantly, such uptake reduction was reversed by FK506 but significantly promoted by PMA. Thus, uptake inhibitions by calcineurin and PKC were additive in CCL39 cells as in cardiomyocytes. However, in cells expressing an NCX1 mutant lacking most of its central loop (NCX1Δ246–672), the uptake rate was not affected by either FK506 or PMA (Fig. 7*a*), indicating that the central loop is required for the effects of calcineurin and PKC.

We then used CCL39 cells not infected with activated CnA to examine the possible interaction of endogenous calcineurin with the β1 repeat deletion mutant (NCX1Δ407–478). In one series, thapsigargin was added to cells 30 min before the uptake measurement to induce a low but sustained $[Ca^{2+}]_i$ increase by reducing the Ca^{2+}-buffering capacity of the endoplasmic reticulum and, thus, activate endogenous calcineurin (Fig. 7*b*), whereas it was not added in another series (Fig. 7*c*). The rate of Na^+_i-dependent $^{45}Ca^{2+}$ uptake in cells expressing wild-type NCX1 was ~50 and 20% higher with 1 μM FK506 in thapsigargin-treated and non-treated cells, respectively, compared with those in the absence of FK506. In contrast, FK506 produced little effect on cells expressing either NCX1Δ407–478

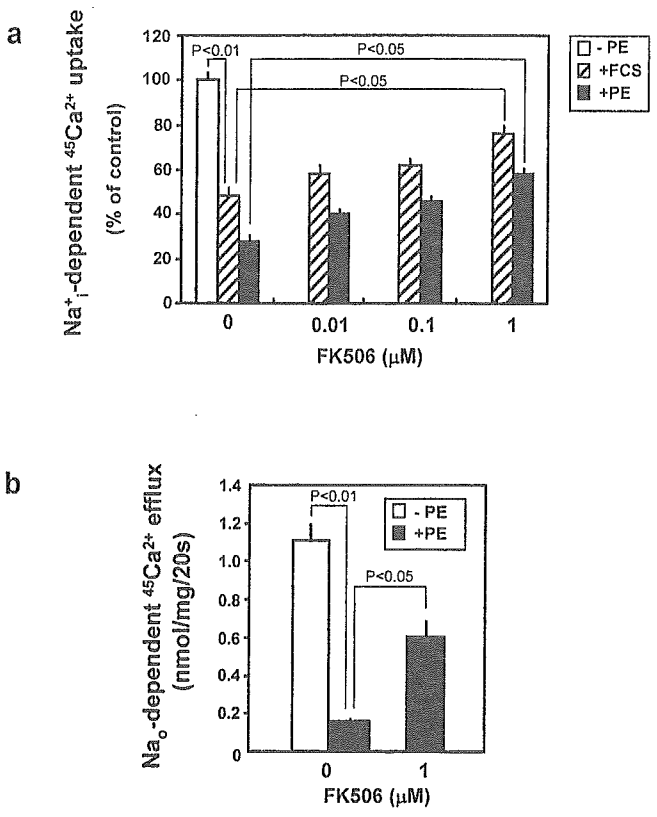

FIG. 4. **Effects of FK506 on Na^+_i-dependent $^{45}Ca^{2+}$ uptake into and Na^+_o-dependent $^{45}Ca^{2+}$ efflux from cardiomyocytes pretreated with PE or FCS.** *a*, myocytes treated with 0 or 10 μM PE or 10% FCS for 72 h (see Fig. 3*a*) were incubated with FK506 for 30 min, and the rates of Na^+_i-dependent $^{45}Ca^{2+}$ uptake were measured. *b*, myocytes were pretreated with PE and FK506 as for *panel a*, and the effect of FK506 on Na^+_o-dependent $^{45}Ca^{2+}$ efflux from PE-treated or non-treated cardiomyocytes were measured. Data in each panel are averages ± S.D. (n = 3).

or NCX1Δ246–672, regardless of thapsigargin treatment (Fig. 7, *b* and *c*). These effects of 1 μM FK506 on NCX activity were significant, suggesting that the β1 repeat is required for the action of endogenous calcineurin.

DISCUSSION

Regulation of Cardiac NCX Activity by Calcineurin and PKC—Recent studies have demonstrated that of the three CnA isoforms, CnAα and CnAβ are expressed in cardiomyocytes, with the latter playing a pivotal role in the induction of cardiac hypertrophy (28, 30). Here, we have provided evidence that the carboxyl tail of CnAβ containing an autoinhibitory domain binds to the β1 repeat of NCX1, one of two internal repeat motifs conserved in the central cytoplasmic loop of NCX family members (31). The β1 repeat constitutes part of the putative Ca^{2+} regulatory site that is responsible for the allosteric regulation of NCX activity by intracellular Ca^{2+} (see review, Ref. 3). Hence, CnAβ binds to a critically important portion of the exchanger. Interestingly, the association of the two proteins was much enhanced in BIO14.6 cardiomyopathic hamster heart (Fig. 2). Furthermore, enhanced association of calcineurin with calmodulin was also observed, suggesting that calcineurin is activated due to a sustained increase in $[Ca^{2+}]_i$ in BIO14.6 cardiomyocytes. Such an interpretation is consistent with our recent report (27).

We used neonatal rat cardiomyocytes treated with 10 μM PE or 10% FCS for 72 h as an *in vitro* hypertrophic model (see Fig. 3*a*). The PE-treated myocytes exhibited typical hypertrophic responses characterized by increased cell size, enhanced sarcomeric organization, and increased ANP expression, although FCS treatment induced less prominent responses (Fig. 3*b*).[2] Importantly, the NCX activity in these hypertrophic myocytes, which was measured as the rate of Na^+_i-dependent $^{45}Ca^{2+}$ uptake or the rate of Na^+_o-dependent Ca^{2+} efflux, was markedly decreased relative to those in non-treated controls (Figs. 3*d* and 4*b*). Such depressed activity was partially reversed by FK506, cyclosporin A, or infection with dominant negative CnA (Figs. 4–6 and "Results"). On the other hand, activated CnA caused a significant decrease in NCX activity in non-treated controls or FCS-treated myocytes, although it had little additional effect on PE-treated cells (Fig. 5). Dominant negative CnA nearly prevented the occurrence of both NCX inhibition and cell hypertrophy in PE- or FCS-treated myocytes (Fig. 5 and "Results"). Therefore, we suggest that calcineurin activity is elevated in PE-treated hypertrophic myocytes as reported previously (28) and that this activity causes NCX inhibition.

PKC inhibitors also caused a partial reversal of depressed NCX activity in PE-treated myocytes (Fig. 6 and "Results"). The effects of the inhibitors of calcineurin and PKC were additive, suggesting that the actions of these enzymes are mutually independent. Importantly, FK506 and calphostin C acted acutely with little influence on myocyte hypertrophic phenotypes. Hence, it is likely that these enzyme actions occur via different mechanisms involving distinct substrate proteins. Of note, however, the PKC-dependent NCX inhibition requires prior activation of calcineurin, because prior infection with dominant negative CnA nearly abolished the PE-induced NCX inhibition (Fig. 5) and because the PKC-dependent NCX inhibition occurred only after the infection of CCL39 cells with activated CnA (Fig. 7*a*).[2] Recent studies (29, 32) have revealed that hypertrophic calcineurin signaling is closely interconnected with activations of PKCα and θ and that PKCα is a necessary mediator of the PE-induced hypertrophy of isolated rat and mouse cardiomyocytes.

The NCX inhibition by calcineurin and PKC seen in PE-treated cardiomyocytes was reproduced in CCL39 cells expressing cloned wild-type NCX1, but not in those expressing NCX1Δ246–672 (Fig. 7*a*), suggesting that the central cytoplasmic loop of NCX1 is required for the effects of calcineurin and PKC. Importantly, this same finding strongly argues against the view that the observed NCX inhibition arose secondarily from changes in cellular conditions, such as altered ion distribution across the plasma membrane. We thus consider that PE alters the functional state of the exchanger causing NCX inhibition. This inhibitory effect of PE, together with the acute NCX stimulation by PE or other agonists of Gαq-coupled receptors reported earlier (8–10), suggests that there exists complex regulatory mechanism(s) for cardiac NCX1.

We observed that the β1 repeat deletion from NCX1 expressed in CCL39 cells abolished the effect of endogenous calcineurin, whereas the deletion of the large cytoplasmic loop abolished the actions of both endogenous calcineurin and recombinant activated CnA (Fig. 7, *a–c*). These data are consistent with the view that NCX1 binding is necessary for the effect of endogenous calcineurin. We speculate that the large cytoplasmic loop of NCX1 may be required to maintain the interaction of calcineurin with its substrate(s). The phosphorylated residues in the cytoplasmic loop might serve as the calcineurin substrate or, alternatively, the cytoplasmic loop could function as a scaffold for ancillary protein(s) that might serve as the substrate. These substrates might be available for the endogenous calcineurin bound to the β1 repeat as well as for the

[2] Y. Katanosaka, S. Wakabaysashi, and M. Shigekawa, unpublished observation.

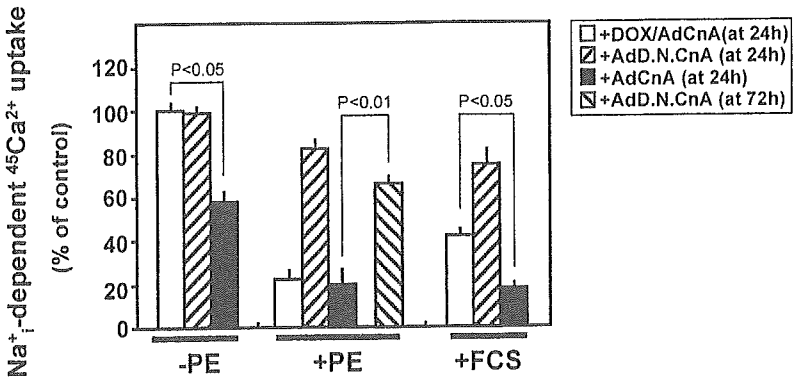

FIG. 5. **Effect of activated or dominant negative CnA on Na^+_i-dependent $^{45}Ca^{2+}$ uptake in cardiomyocytes pretreated with PE or FCS.** Myocytes were treated with no growth factor (*−PE*), 10 μM PE (*+PE*), or 10% FCS (*+FCS*) for 72 h. In one series (*bar* on the *extreme right* for *+PE*), PE-treated myocytes were subsequently infected with dominant negative can, and the rate of Na^+_i-dependent $^{45}Ca^{2+}$ uptake was measured 24 h later. In all other series, myocytes were infected at 24 h after the start of growth factor treatment either with activated CnA in presence (*+DOX/AdCnA*) or absence (*+AdCnA*) of DOX or with dominant negative CnA (*+AdD.N.CnA*), and uptake rates were measured 48 h later. The uptake rate in the *−PE+DOX/AdCnA* series was taken as 100%. Data are averages ± S.D. (n = 3).

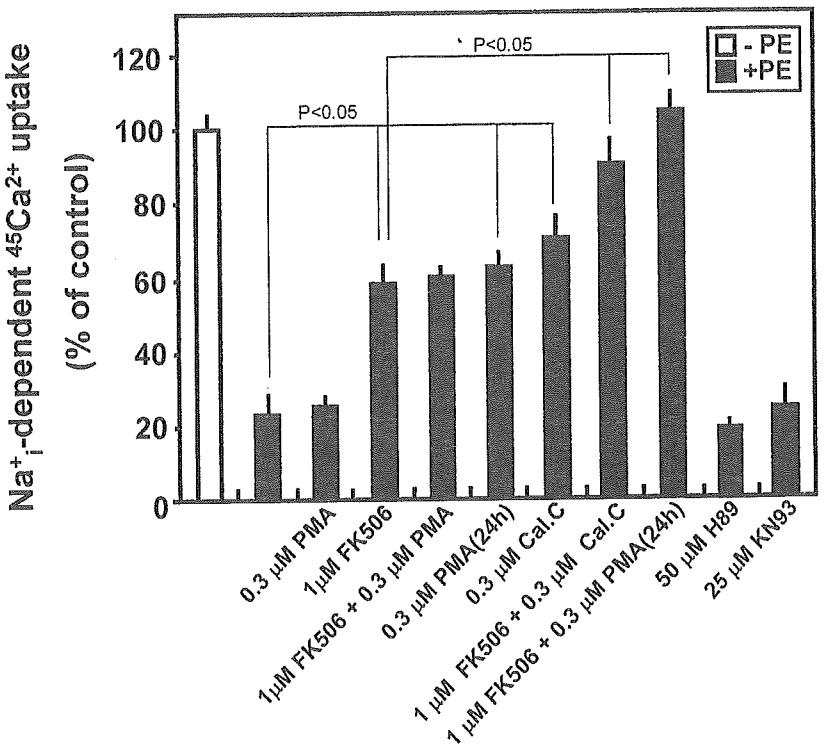

FIG. 6. **Effects of FK506, protein kinase modulators and their combinations on Na^+_i-dependent $^{45}Ca^{2+}$ uptake into PE-treated cardiomyocytes.** Myocytes were incubated with the indicated agents during the last 30 min of a 72-h treatment with 0 or 10 μM PE, and then the rates of Na^+_i-dependent $^{45}Ca^{2+}$ uptake were measured. In some series, myocytes were incubated with 0.3 μM PMA during the last 24 h of PE treatment (*PMA(24h)*). *Cal.C*, calphostin C. Data are averages ± S.D. (n = 3).

recombinant activated CnA overexpressed in myocytes, although this may not happen when the large cytoplasmic loop is deleted. It is noteworthy, however, that activated CnA, lacking its C-terminal tail and the ability to bind to the NCX1 β1 repeat, was able to regulate NCX activity (Fig. 5). Thus, in view of the limitations inherent in these mutation studies, we cannot rule out the possibility that calcineurin may inhibit NCX activity without binding to NCX1. Further studies are required to establish the causal relationship between calcineurin binding and NCX inhibition.

Pathological Relevance of Depressed NCX Function—Myocardial hypertrophy occurs in response to a variety of stimuli, including the chronic activation of $G\alpha^q$ class of G-proteins that leads to the activation of calcineurin, PKC, and mitogen-activated protein kinases (15). On the other hand, calcineurin and its primary downstream effector, the nuclear factor of activated T cells (NFAT), have been shown to be important mediators of *in vitro* and *in vivo* cardiac hypertrophic responses (see reviews, Refs. 15 and 16). The exact mechanism by which calcineurin promotes pathological hypertrophic responses is currently unknown, as few targets for calcineurin other than the NFATs that contribute to the development of cardiac hypertrophy have been identified. This study has provided evidence suggesting that NCX1 may be one of such targets for calcineurin. The results shown here are in good agreement with the recent report by Wang *et al.* (33) showing that NCX current density was significantly reduced in hypertrophic cardiomyocytes isolated from aortic banded mice, whereas this did not occur in mice receiving daily cyclosporin A injection during aortic constriction. Because depressed NCX activity is likely to cause the chronic elevation of $[Ca^{2+}]_i$ in cardiomyocytes, depressed NCX activity might play an important role in the development of myocardial hypertrophy and the subsequent contractile dysfunction. However, the pathological significance of depressed NCX activity needs to be established in future studies, as enhanced NCX1 expression and function have also

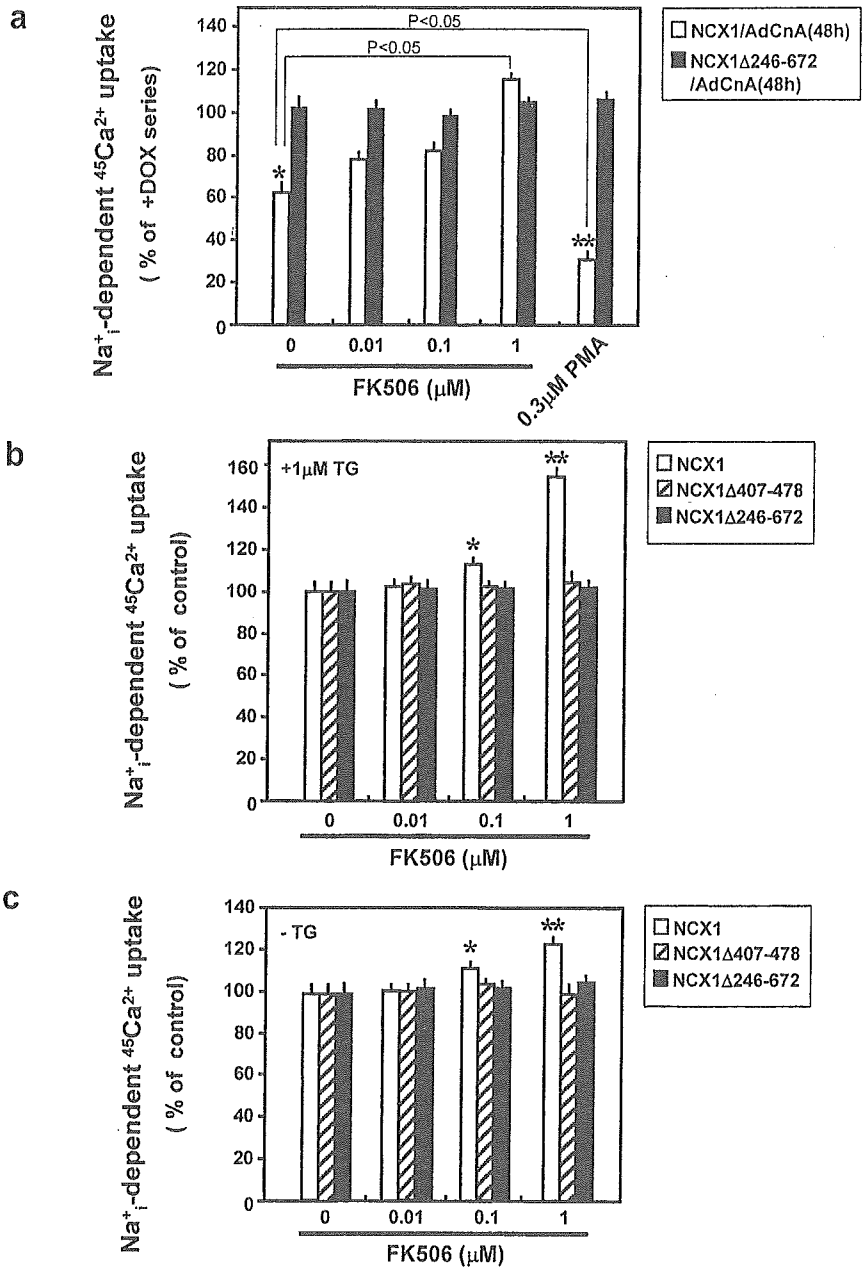

FIG. 7. **Effect of FK506 or PMA on Na^+_i-dependent $^{45}Ca^{2+}$ uptake into CCL39 cells expressing NCX1 variants and/or activated CnA.** *a*, cells expressing wild-type NCX1 or NCX1Δ246–672 were infected with activated CnA (*AdCnA*) for 48 h in the presence or absence of 1 μM DOX. The cells were then incubated with the indicated concentrations of FK506 or PMA for 30 min, and the rates of Na^+_i-dependent $^{45}Ca^{2+}$ uptake were measured. The uptake rate in the series with activated CnA in the presence of DOX (+DOX/AdCnA) was taken as 100%. *b*, cells expressing wild-type NCX1, NCX1Δ407–478, or NCX1Δ246–672 were incubated with 1 μM thapsigargin (*TG*) and the indicated concentrations of FK506 for 30 min, and the uptake rates were measured. *c*, the uptake rate was measured as for *panel b*, except that thapsigargin was omitted. In *panels b* and *c* the uptake rate with no FK506 was taken as 100% for each NCX variant. Data are averages ± S.D. ($n = 9$). *, $p < 0.05$ *versus* control; **, $p < 0.01$ *versus* control.

been reported for cardiomyocytes isolated from some animal models of cardiac hypertrophy and heart failure (6, 7).

REFERENCES

1. Bridge, J. H. B., Smolley, J. R., and Spitzer, K. W. (1990) *Science* **248,** 376–378
2. Bers, D. M. (2000) *Circ. Res.* **87,** 275–281
3. Shigekawa, M., and Iwamoto, T. (2001) *Circ. Res.* **88,** 864–876
4. Kent, R. L., Rozich, J. D., McCollam, P. L., McDemott, D. E., Thacker, U. F., Menick, D. R., McDermott, P. J., and Cooper, G., IV (1993) *Am. J. Physiol.* **265,** H1024–H1029
5. Studer, R., Reinecke, H., Biger, J., Eschenhagen, T., Böhm, M., Hasenfuss, G., Just, H., Holtz, J., and Drexler, H. (1994) *Circ. Res.* **75,** 443–453
6. Ahmmed, G. U., Dong, P. E., Song, G., Ball, N. A., Xu, Y., Walsh, R. A., and Chiamvimonvat, N. (2000) *Circ. Res.* **86,** 558–570
7. O'Rourke, B., Kass, D. A., Tomaselli, G. F., Kääb, S., Tunin, R., and Marbán, E. (1999) *Circ. Res.* **6,** 558–570
8. Iwamoto, T., Pan, Y., Wakabayashi, S., Imagawa, T., Yamanaka, H. I., and Shigekawa, M. (1996) *J. Biol. Chem.* **271,** 13609–13615
9. Iwamoto, T., Pan Y., Nakamura, T. Y., Wakabayashi, S., and Shigekawa, M. (1998) *Biochemistry* **37,** 17230–17238
10. Stengl, M., Mubagwa, K., Carmeliet, E., and Flameng, W. (1998) *Cardiovasc. Res.* **38,** 703–710
11. Link, B., Qiu, Z., He, Z., Tong, Q., Hilgemann, D.W., and Philipson, K.D. (1998) *Am. J. Physiol.* **274,** C415–C423
12. Wei, S.-K., Ruknudin, A., Hanlon, S. U., McCurley, J. M., Schulze, D. H., and Haigney, M. C. P. (2003) *Circ. Res.* **92,** 897–903
13. Condrescu, M., Hantash, B. M., Fang, Y., and Reeves, J. P. (1999) *J. Biol. Chem.* **274,** 33279–33286
14. Molkentin, J. D., Lu, J.-R., Antos, C. L., Markham, B., Richardson, J., Robins, J., Grant, S. R., and Olson, E. N. (1998) *Cell* **93,** 215–228
15. Molkentin, J. D., and Dorn, G. W., II (2001) *Ann. Rev. Physiol.* **63,** 391–426
16. Vega, R. B., Bassel-Duby, R., and Olson, E. N. (2003) *J. Biol. Chem.* **278,** 36981–36984
17. Simpson, P., McGrath, A., and Savion, S. (1982) *Circ. Res.* **51,** 787–801
18. Shibasaki, F., and MacKeon, F. (1995) *J. Cell Biol.* **131,** 735–743
19. Wang, H.-G., Pathan, N., Ethell, I. M., Krajewski, S., Yamaguchi, Y., Shibasaki, F., Mckeon, F., Bobo, T., Franke, T. F., and Reed, J. C. (1999) *Science* **284,** 339–343
20. Laemmli, U. K. (1970) *Nature* **227,** 680–685
21. Tawada-Iwata, Y., Imagawa, T., Yoshida, A., Takahashi, M., Nakamura, H., and Shigekawa, M. (1993) *Am. J. Physiol.* **264,** H1447–H1453
22. Pan ,Y., Iwamoto, T., Uehara, A., Nakamura, T. Y., Imanaga, I., and Shigekawa, M. (2000) *Am. J. Physiol.* **279,** C393–C402
23. Furukawa, K., Tawada, Y., and Shigekawa, M. (1988) *J. Biol. Chem.* **263,** 8058–8065
24. Saito, S., Hiroi, Y., Zou, Y., Aikawa, R., Toko, H., Shibasaki, F., Yazaki, Y., Nagai, R., and Komuro, I. (2000) *J. Biol. Chem.* **275,** 34528–34533
25. Bajusz, E., Homburger, F., Baker, J. R., and Bogdonoff, P. (1969) *Ann. N. Y. Acad. Sci.* **156,** 396–420
26. Nigro, V., Okazaki, Y., Belsito, A., Piluso, G., Matsuda, Y., Politano, L., Nigro, G., Ventura, C., Abbondanza, C., Molinari, A. M., Acampora, D., Nishimura,

M., Hayashizaki, Y., and Puca, G. A. (1997) *Hum. Mol. Genet.* **6,** 601–607
27. Iwata, Y., Katanosaka, Y., Arai, Y., Komamura, K., Miyatake, K., and Shigekawa, M. (2003) *J. Cell Biol.* **161,** 957–967
28. Taigen, T., De Windt, L. J., Lim, H. W., and Molkentin, J. D. (2000) *Proc. Natl. Acad. Sci. U. S. A.* **97,** 1196–1201
29. De Windt, L. J., Lim, H. W., Haq, S., Force, T., and Molkentin, J. D. (2000) *J. Biol. Chem.* **275,** 13571–13579
30. Bueno, O. F., Wilkins, B. J., Tymitz, K. M., Glascock, B. J., Kimball, T. F., Lorenz, J. N., and Molkentin, J. D. (2002) *Proc. Natl. Acad. Sci. U. S. A.* **99,** 4586–4991
31. Schwarz, E. M., and Benzer, S. (1997) *Proc. Natl. Acad. Sci. U. S. A.* **94,** 10249–10254
32. Braz, J. C., Bueno, O. F., De Windt, L. J., and Molkentin, J. D. (2002) *J. Cell Biol.* **156,** 905–919
33. Wang, Z., Nolan, B., Kutschke, W., and Hill, J. A. (2001) *J. Biol. Chem.* **276,** 17706–17711

Original Article

Association of Genetic Polymorphisms of Sodium-Calcium Exchanger 1 Gene, *NCX1*, with Hypertension in a Japanese General Population

Yoshihiro KOKUBO*[1], Nozomu INAMOTO*[1], Hitonobu TOMOIKE*[1], Kei KAMIDE*[2], Shin TAKIUCHI*[2], Yuhei KAWANO*[2], Chihiro TANAKA*[3], Yuki KATANOSAKA*[3], Shigeo WAKABAYASHI*[3], Munekazu SHIGEKAWA*[3], Otosaburo HISHIKAWA*[4], and Toshiyuki MIYATA*[3]

The Na^+/Ca^{2+} exchanger (NCX) is a membrane protein involved in calcium homeostasis, catalyzing the exchange of one Ca^{2+} ion for three Na^+ ions across the cell membrane. The Na^+/Ca^{2+} exchange has been suggested to play a role in the pathogenesis of hypertension. Therefore, we examined whether genetic variations in *NCX1* were associated with hypertension. Among 15 polymorphisms identified in 96 hypertensive subjects by sequencing the entire exon and promoter regions of *NCX1*, 7 representative polymorphisms with a minor allele frequency of greater than 4% were genotyped in 1,865 individuals, of whom 787 were hypertensive and 1,072 were normotensive. These subjects were residents of Suita City and were randomly selected as a population for the Suita cohort study. Multivariate logistic regression analysis performed after adjusting for age, body mass index, hyperlipidemia, diabetes mellitus, smoking, and drinking revealed that the −23200T>C and −23181T>C polymorphisms in the 5′ upstream region of exon 1c were significantly associated with hypertension in men (−23200T>C: CC *vs.* TC+TT: odds ratio=0.61; 95% confidence intervals: 0.39 to 0.97; p=0.04) and in women (−23181T>C: CC *vs.* TC+TT: odds ratio=1.45; 95% confidence intervals: 1.04 to 2.02; p=0.03), respectively. Thus, our study suggests that *NCX1* is one of the genes related to susceptibility to essential hypertension in the Japanese general population.
(*Hypertens Res* 2004; 27: 697–702)

***Key Words*: NCX1, Na^+/Ca^{2+} exchanger, gene variants, hypertension**

Introduction

The Na^+/Ca^{2+} exchanger (NCX) is an important membrane protein involved in calcium homeostasis in various cell types and catalyzes the electrogenic exchange of one Ca^{2+} ion for three Na^+ ions across the plasma membrane (*1–3*). The Na^+/Ca^{2+} exchange has been well demonstrated to play a role in the pathogenesis of hypertension. Blaustein *et al.* suggested that excessive Na^+ retention may secrete an ouabain-like substance that increases the cytosolic Na^+ concentration by inhibiting the plasmalemmal Na^+-pump, which increases the cytosolic Ca^{2+} concentration ($[Ca^{2+}]_i$) by reducing Ca^{2+}-extrusion *via* Na^+/Ca^{2+} exchange (*4–6*). The increase in arteri-

From the *[1]Division of Preventive Cardiology, *[2]Division of Hypertension and Nephrology, and *[3]Research Institute, National Cardiovascular Center, Suita, Japan, and *[4]Suita City Medical Association, Suita, Japan.

This study was supported by the Program for Promotion of Fundamental Studies in Health Science of the Pharmaceuticals and Medical Devices Agency (PMDA) of Japan MPJ-3.

Address for Reprints: Yoshihiro Kokubo, M.D., Ph.D., Division of Preventive Cardiology, National Cardiovascular Center, 5-7-1 Fujishiro-dai, Suita 565-8565, Japan. E-mail: ykokubo@hsp.ncvc.go.jp

Received March 2, 2004; Accepted in revised form June 4, 2004.

Table 1. Basic Characteristics of Subjects in Suita, a Japanese Urban Population, 2002

	Men (n=858)	Women (n=1,007)
Age (year)	66.3±11.1*	63.3±11.0*
Systolic blood pressure (mmHg)	131.9±19.5*	128.0±19.6*
Diastolic blood pressure (mmHg)	79.7±10.7*	76.6±10.7*
Body mass index (kg/m^2)	23.3±3.0*	22.3±3.2*
Total cholesterol (mmol/l)	5.10±0.78	5.57±0.79*
HDL-cholesterol (mmol/l)	1.42±0.36	1.67±0.40*
Current smokers (%)	30.1†	6.3†
Current drinkers (%)	67.0†	29.3†
Present illness (%)		
Hypertension	47.4†	38.2
Hyperlipidemia	27.4	55.2†
Diabetes mellitus	12.6†	5.2

Values are mean±SD or percentage. Hypertension indicates systolic blood pressure ≥140 mmHg and/or diastolic blood pressure ≥90 mmHg or antihypertensive medication; hyperlipidemia, total cholesterol ≥5.68 mmol/l (220 mg/dl) or antihyperlipidemia medication; diabetes, fasting plasma glucose ≥7.0 mmol/l (126 mg/dl) or non-fasting plasma glucose ≥11.1 mmol/l (200 mg/dl) or HbA1c ≥6.5% or antidiabetic medication. * $p<0.05$ between women and men by Student's t-test. † $p<0.05$ between women and men by χ^2 test. HDL, high-density lipoprotein.

al tone caused by high $[Ca^{2+}]_i$ would thus result in an elevation of blood pressure. Indeed, several previous studies have reported that Na^+/Ca^{2+} exchange activity was altered in the renal arterioles or arterial smooth muscle of spontaneous or salt-sensitive hypertensive rats (*7–11*). However, it is unknown whether such a mechanism relates to the occurrence of essential hypertension.

Of three isoforms (NCX1–3) derived from different genes, NCX1 is predominantly expressed in the heart, neurons and renal tubules, but is expressed at lower levels in other tissues, including the smooth muscle, skeletal muscle, lung and spleen (*1–3*). The *NCX1* gene (*SLC8A1*) is located on human chromosome 2p22.1 and includes 12 exons (*12*). There are at least 12 splice variants generated in different combinations from six exons in a tissue-specific manner (*13*). In addition, five exons encode 5′-untranslated sequences that are under the control of three tissue-specific promoters (*14–17*).

This study was undertaken to identify genetic variations in *NCX1* in a group of hypertensive subjects, and to examine the association of these variations with the presence of hypertension in a general population. In contrast to other association studies, which often focus on a limited number of polymorphisms in a gene, our study evaluated the full array of coding- and promoter-sequence polymorphisms in *NCX1*.

Methods

Subjects of the Suita Population Study

The subjects of the Suita study consisted of 14,200 men and women (30 to 79 years of age), who had been randomly selected from the municipal population registry and stratified by in consideration of gender and age (stratified in 10-year intervals). They were all invited, by letter, to receive medical and behavioral examinations every 2 years at the Division of Preventive Cardiology, National Cardiovascular Center, Japan. DNA from the leukocytes was collected from participants who visited the National Cardiovascular Center between May 2002 and February 2003. All of the participants were Japanese. Only those who gave written informed consent for genetic analyses were included in this study. The study protocol was approved by the Ethical Review Committee of the National Cardiovascular Center. In this study, the genotypes of 1,865 samples were determined. The characteristics of 1,865 participants (858 men, 1,007 women) are shown in Table 1. Routine blood examinations that included total serum cholesterol, high-density lipoprotein (HDL) cholesterol, triglyceride, and glucose levels were performed. A physician or nurse interviewed each patient in regard to smoking and drinking habits and personal history of cardiovascular disease, including angina pectoris, myocardial infarction, and/or stroke.

Blood pressure was measured in a sitting position after at least 10 min of rest. Systolic and diastolic blood pressures (SBP/DBP) were taken as the means of two measurements recorded more than 3 min apart by well-trained doctors. Hypertension was defined as SBP of ≥140 mmHg, DBP of ≥90 mmHg, or the current use of antihypertensive medication (*18*). Diabetes mellitus was defined as fasting plasma glucose ≥7.0 mmol/l (126 mg/dl), non-fasting plasma glucose ≥11.1 mmol/l (200 mg/dl), current use of antidiabetic medication, or HbA1c ≥6.5%. Hyperlipidemia was defined as total cholesterol ≥5.68 mmol/l (220 mg/dl) or current use of antihyperlipidemia medication. Body mass index (BMI)

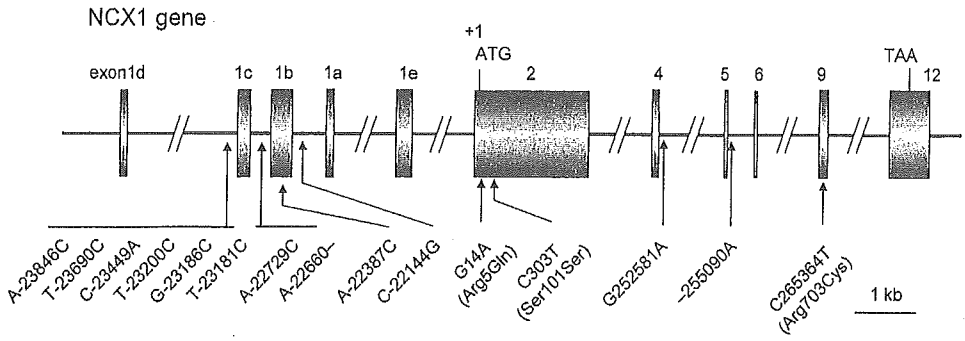

Fig. 1. *Genome structure of human* NCX1. *The* NCX1 *gene consists of sixteen exons, five (exons 1a–1e) of which direct tissue-specific transcription and eleven (exons 2–12) of which encode the open reading frame (17). The five tissue-specific transcription exons (exons 1a–1e) and the exons in which the SNPs were identified are depicted. The nucleotide changes and amino acid substitutions are also shown. The A of the ATG of the initiator Met codon is denoted nucleotide +1.*

was calculated as weight (in kg) divided by height (in m) squared.

Direct Sequencing for Single Nucleotide Polymorphism (SNP) Discovery and Genotyping of Polymorphisms

For DNA sequencing, 96 patients with essential hypertension were recruited from the Division of Hypertension and Nephrology, National Cardiovascular Center, Japan. The method of direct sequencing was described previously (*19*). Fifteen polymorphisms were identified by sequencing and 7 representative polymorphisms with a minor allele frequency of greater than 4% were genotyped by the TaqMan-polymerase chain reaction (PCR) system (*20*). Only those who gave written informed consent for genetic analyses were included in this study. The study protocol was approved by the Ethical Review Committee of the National Cardiovascular Center.

Statistical Analysis

Analysis of variance was used to compare mean values between groups, and if overall significance was demonstrated, the intergroup difference was assessed by means of a general linear model. Frequencies were compared by χ^2 analysis.

Logistic regression analyses were used to examine the association between the genotypes and blood pressure in each sex with consideration for potential confounding risk variables, including age, BMI, present illness (hyperlipidemia and diabetes mellitus), lifestyle (smoking and drinking), and antihypertensive medication. For multivariate risk predictors, the adjusted odds ratios were given with 95% confidence intervals. The relationship between genotype and risk of hypertension was expressed in terms of the odds ratios adjusted for possible confounding effects including age, BMI, present illness (hyperlipidemia and diabetes mellitus), and lifestyle (smoking and drinking). SAS statistical software (release 8.2; SAS Institute, Cary, USA) was used for statistical analyses (*21*).

Results

Basic Characteristics of Subjects in the Suita Study

The characteristics of the 1,865 participants (858 men, 1,007 women) are summarized in Table 1. Age, SBP, DBP, BMI, percentage of current smokers, percentage of current drinkers, and prevalence of hypertension and diabetes mellitus were significantly higher in men than in women. Total cholesterol, HDL-cholesterol, and percentage of hyperlipidemia were significantly higher in women than in men.

Polymorphisms of *NCX1*

The *NCX1* gene has a complicated genome structure containing five alternative 5′ exons producing separate tissue-specific promoters and six exons encoding open reading frames (Fig. 1). We sequenced the entire exon and promoter regions of *NCX1* from 96 patients (182 alleles) with hypertension, and identified 15 polymorphisms (Table 2, Fig. 1). We identified two missense mutations, Arg5Gln in exon 2 and Arg703Cys in exon 9, in *NCX1* (Table 2). Each of the missense mutations was identified in one out of 96 individuals, indicating that their allele frequencies were rare. Two SNPs, −23200T>C and −23186G>C, were in linkage disequilibrium. Seven representative polymorphisms with a minor allele frequency of greater than 4% were genotyped for the association study.

Susceptible SNPs Related to Hypertension

Seven polymorphisms in *NCX1* were genotyped in 1,865 individuals, of whom 787 were hypertensive and 1,072 were normotensive. The primers and probes of the TagMan-PCR system and the genotyping results are summarized in Table

Table 2. List of 15 Polymorphisms and Their Allele Frequencies in the *NCX1* Gene Identified by Direct Sequencing

Allele 1/Allele 2 SNPs	TaqMan typing	Amino acid change	Region	Allele 1 Homo	Hetero	Allele 2 Homo	Total	Allele frequency Allele 1	Allele frequency Allele 2	Flanking sequence
−23846A>C			intron 1d	94	1	0	95	0.995	0.005	tcacactgcctt[a/c]aattcagggact
−23690T>C	typing		intron 1d	62	31	2	95	0.816	0.184	aaatttaactta[t/c]agcaaggaaaga
−23449C>A	typing		intron 1d	85	9	1	95	0.942	0.058	catactcacatt[c/a]atgtttgaggag
−23200T>C*	typing		intron 1d	0	9	86	95	0.047	0.953	attccgcccccct[t/c]tttgttgcggag
−23186G>C*			intron 1d	0	9	86	95	0.047	0.953	ttgttgcggagg[g/c]aaactgaggttc
−23181T>C	typing		intron 1d	18	57	20	95	0.489	0.511	gcggaggcaaac[t/c]gaggttcctgga
−22729A>C	typing		intron 1c	71	23	1	95	0.868	0.132	taattatgagga[a/c]agtgatttattg
−22660delA			intron 1c	94	1	0	95	0.995	0.005	gattgctgcatt[a/−]ggtttttccca
−22387A>C		5′ UTR	exon 1b	93	3	0	96	0.984	0.016	attaaaaaaaaa[a/c]tcattgatatat
−22144C>G	typing		intron 1b	84	9	2	95	0.932	0.068	gcgcggccacaa[c/g]gcactgcgggggc
14G>A		Arg5Gln	exon 2	95	1	0	96	0.995	0.005	tgtacaacatgc[g/a]gcgattaagtct
303C>T		Ser101Ser	exon 2	95	1	0	96	0.995	0.005	tcggttcatgtc[c/t]tctatagaagtc
252581G>A	typing		intron 4	45	40	11	96	0.677	0.323	tcttctctctcc[g/a]tgtctccctact
255089–255090insA			intron 5	94	1	0	95	0.995	0.005	tcaggtgataca[−/a]gtagctctgtga
265364C>T		Arg703Cys	exon 9	95	1	0	96	0.995	0.005	gcagaaatgggg[c/t]gccccatcctgg

The A of the ATG of the initiator Met codon is denoted nucleotide +1. * The apparent linkage disequilibrium ($r^2 \geq 0.5$). NCX1, Na^+/Ca^{2+} exchanger; SNP, single nucleotide polymorphism.

3. Multivariate logistic regression analysis after adjusting for confounding risk variables such as age, BMI, hyperlipidemia, diabetes mellitus, smoking, and drinking, revealed that two polymorphisms, −23200T>C and −23181T>C, in the 5′ upstream region of exon 1c were significantly associated with hypertension in men (−23200T>C: CC *vs.* TC+TT: odds ratio=0.61; 95% confidence interval: 0.39 to 0.97; $p=0.04$) and in women (−23181T>C: CC *vs.* TC+TT: odds ratio=1.45; 95% confidence interval: 1.04 to 2.02; $p=0.03$), respectively (Table 4). When normotension was defined as SBP ≤120 mmHg, DBP ≤80 mmHg, and the absence of anti-hypertensive medication, and hypertension was defined as SBP ≥160 mmHg, DBP ≥100 mmHg, or the current use of antihypertensive medication, −23200T>C polymorphism was significantly associated with hypertension in men (CC *vs.* TC+TT: odds ratio=0.42; 95% confidence interval: 0.20 to 0.92; $p=0.03$) after adjusting for the confounding factors described above.

Discussion

In this study, we sequenced the exon and promoter regions of *NCX1* and identified 15 polymorphisms. Seven representative polymorphisms were genotyped from 1,865 subjects to examine the association of hypertension with *NCX1*. After adjustment for various confounding factors, we identified that the −23200T>C polymorphism in the 5′ upstream region of exon 1c was significantly associated with hypertension in men and the −23181T>C polymorphism in the 5′ upstream region of exon 1c was significantly associated with hypertension in women.

The *NCX1* gene has at least 12 splice variants generated in different combinations from six exons in a tissue-specific manner (*13*). In addition, three exons encode 5′-untranslated sequences that are under the control of three tissue-specific promoters (*14–16*). Exon 1c is a part of the "heart" specific transcript (*17*) and its upstream region is not likely a promoter. Therefore, the −23200T>C and −23181T>C polymorphisms present in the upstream region of exon 1c are not likely to be directly involved in transcription of *NCX1*. Rather, these polymorphisms may be in linkage disequilibrium with other polymorphisms in the region that were not examined by sequencing in this study.

In this study, the −23200T>C polymorphism in men and −23181T>C polymorphism in women were identified as SNPs conferring susceptibility for hypertension. It is well known that the greater incidence of hypertension and coronary artery disease in men is, in part, related to gender differences in possible vascular protective effects of the female sex hormones estrogen and progesterone. Furthermore, NCX1 might be related to salt-sensitive hypertension (*22*). Since there is a gender difference in salt-sensitivity and plasma renin activity (*23*, *24*), −23200T>C and −23181T>C in *NCX1* may be linked with unidentified causative genetic variations that would be influenced by the female sex hormones and/or salt-sensitivity.

In this study, we identified two missense mutations, Arg5Gln in exon 2 and Arg703Cys in exon 9, in *NCX1*. Arg5 is located within the signal peptide sequence consisting of the first N-terminal 35 amino acids of NCX1, which are removed during biosynthesis (*1*). We expressed a mutant canine NCX1 with the Arg5Gln substitution in the fibroblastic

Table 3. Genotyping Conditions and Results of *NCX1* Polymorphisms in 1,818 Individuals by TaqMan-PCR Method

SNP	Primer	Probe	Genotypes results
−23690T>C	CTCTCCCCACAGGTCATTCTG	Fam-ATTTAACTTATAGCAAGGAA-MGB	(TT/TC/CC)
	GCAGGAATCGTTCTTGCCTAA	Vic-TTAACTTACAGCAAGGAA-MGB	=(1,140/590/88)
−23449C>A	GAATCTGCAATCCCCATGTGAT	Fam-CTCACATTCATGTTTGAG-MGB	(CC/CA/AA)
	AGAACCACTGCTCTAGGCCAAT	Vic-ACTCACATTAATGTTTGAGG-MGB	=(1,542/261/15)
−23200T>C	TTCTGAGGTGCAAGGAGGGTT	Fam-CCCCCTTTTTGTTGC-MGB	(TT/TC/CC)
	GGCAGTCACCACGACTGATAGA	Vic-CCCCCTCTTTGTTG-MGB	=(4/196/1,618)
−23181T>C	GGCAGTCACCACGACTGATAGA	Fam-TCCAGGAACCTCAGTTT-MGB	(TT/TC/CC)
	AGGCTATTTCTTCCATTCCGC	Vic-CCAGGAACCTCGGTTT-MGB	=(503/869/446)
−22729A>C	GCCTGGTGCAGTGTTCCTTTA	Fam-ATTATGAGGAAAGTGATTTA-MGB	(AA/AC/CC)
	GCCCTTTCCAAGAGAAGCATTA	Vic-TATGAGGACAGTGATTTA-MGB	=(1,369/406/43)
−22144C>G	AAAAGAAAAGTTGCAGCGCCT	Fam-CCACAACGCACTGC-MGB	(CC/CG/GG)
	TTTTTCGATTTCCTGCCGG	Vic-CACAAGGCACTGCG-MGB	=(1,687/131/0)
252581G>A	AAACAAAGACATACCAGCGAGAAA	Fam-CTCTCTCCGTGTCTC-MGB	(GG/GA/AA)
	AAATTGCTAAAGCTTCAAAGGCA	Vic-TCTCTCCATGTCTCC-MGB	=(823/798/197)

PCR, polymerase chain reaction; SNP, single nucleotide polymorphism.

Table 4. Odds Ratio of −23200T>C Polymorphism in Men and −23181T>C Polymorphism in Women*

Gender	SNP	OR (95% CI)		*p*	OR (95% CI)		*p*
Men	−23200T>C	CC	1 (reference)		CC+TC	1 (reference)	
		TC+TT	0.61 (0.39–0.97)	0.04	TT	—	—
Women	−23181T>C	CC	1 (reference)		CC+TC	1 (reference)	
		TC+TT	1.45 (1.04–2.02)	0.03	TT	1.39 (1.00–1.92)	0.05

*Conditional logistic analysis, adjusted for age, body mass index, present illness (hyperlipidemia and diabetes mellitus), and lifestyle (smoking and drinking). SNP, single nucleotide polymorphism; OR, odds ratio; CI, confidence intervals.

cell line CCL39, and found that this mutant NCX1 was properly targeted into the plasma membrane and exhibited the normal Na^+/Ca^{2+} exchange activity (unpublished observations), consistent with previous reports stating that signal sequence is not essential for functional expression of the NCX1 protein (*25*, *26*). On the other hand, Arg703 is located within the large cytoplasmic loop connecting the transmembrane segments 5 and 6, which are not essential for the functional expression of the NCX1 protein (*1*). Thus, the two rare mutations identified in this study would not grossly impair the function of NCX1.

In summary, we showed that the SNPs −23200T>C and −23181T>C in *NCX1* were associated with hypertension. The pathophysiological functional behaviors of these polymorphisms remain to be clarified. In future studies, it will be necessary to clarify the function of these polymorphisms or to identify the causative polymorphisms that are in linkage disequilibrium with these polymorphisms.

Acknowledgements

We would like to express our highest gratitude to Dr. Soichiro Kitamura, President of the National Cardiovascular Center, for his support of the Millennium genome project (MPJ-3). We would also like to thank Dr. Katsuyuki Kawanishi, Dr. Toshifumi Mannami, and Mr. Tadashi Fujikawa for their continuous support of our population survey in Suita City. We also thank the members of the Satsuki-Junyukai. We also thank all the staff in the Division of Preventive Cardiology for supporting medical examination and M. Banno, Y. Tokunaga, and C. Imai for their technical assistance. Finally, we are grateful to Dr. Tetsuji Yokoyama for his statistical advice.

References

1. Philipson KD, Nicoll DA: Sodium-calcium exchange: a molecular perspective. *Annu Rev Physiol* 2000; **62**: 111–133.
2. Shigekawa M, Iwamoto T: Cardiac Na^+-Ca^{2+} exchange: molecular and pharmacological aspects. *Circ Res* 2001; **88**: 864–876.
3. Blaustein MP, Lederer WJ: Sodium/calcium exchange: its physiological implications. *Physiol Rev* 1999; **79**: 763–854.
4. Blaustein MP: Sodium ions, calcium ions, blood pressure regulation, and hypertension: a reassessment and a hypothesis. *Am J Physiol* 1977; **232**: C165–C173.
5. Blaustein MP: Physiological effects of endogenous ouabain: control of intracellular Ca^{2+} stores and cell respon-